Inter-domain flexibility and AI-guided sequence optimization enhance de novo enzyme function

Paula Wagner Egea[1,#], Florent Delhommel,[2,3,#] Ghulam Mustafa[1], Florian Leiss-Maier[1], Lisa Klimper,[1] Thomas Badmann,[1] Anna Heider,[1] Idoia Wille,[1] Michael Groll[1], Michael Sattler,[2,3] Cathleen Zeymer[1,4,*]

[1] Center for Functional Protein Assemblies & Department of Bioscience, TUM School of Natural Sciences, Technical University of Munich (TUM), 85748 Garching, Germany
[2] Bavarian NMR Center & Department of Bioscience, TUM School of Natural Sciences, Technical University of Munich (TUM), 85748 Garching, Germany
[3] Institute of Structural Biology, Molecular Targets and Therapeutics Center, Helmholtz Munich, 85764 Neuherberg, Germany
[4] TUM Catalysis Research Center, Technical University of Munich (TUM), 85748 Garching, Germany

* E-mail: cathleen.zeymer@tum.de

[#] These authors contributed equally.

Table of contents

List of Tables

List of Figures

S1–MOLECULAR CLONING AND SEQUENCES

S1.1–Molecular cloning

Synthetic genes were ordered from Twist Bioscience (South San Francisco, CA, USA). All PCR reactions were performed as described in **Table S–I** and **Table S–II** using primers described in **Table S–III**. All vectors were assembled using an isothermal Gibson Assembly (1 h, 50 °C). Single point mutations were introduced according to the QuikChange protocol from New England Biolabs Q5 High-Fidelity DNA Polymerase protocol or Site-directed Ligase-Independent Mutagenesis (SLIM) method [1] with the corresponding primers for the point mutation (**Table S–III**).

Table S–I. Composition of PCR reactions.

Component	Amount	Final concentration
dNTPs (10 mM)	1 µL	0.2 mM
Template DNA (100 ng/µL)	1 µL	2 ng/µL
Primer for (10 mM)	2.5 µL	0.5 mM
Primer rev (10 mM)	2.5 µL	0.5 mM
Q5 buffer (5x)	10 µL	1x
Q5 High-Fidelity polymerase	1 µL	–
DMSO	1.5 µL	3 %
add ddH$_2$O with 6% glycerol (v/v), 0.01% bromophenol blue (w/v)	to 50 µL	

Amplification of the fragments and linearized vectors was confirmed by agarose gel electrophoresis. DpnI digestion (37 °C, 1 h or overnight) was performed to remove methylated template DNA from PCR-amplified products. The purification of those products was achieved either by using the PCR Purification Kit (Jena Bioscience GmbH, Jena, Germany) or after agarose gel electrophoresis from respective bands using the Monarch DNA Gel Extraction Kit (New England Biolabs GmbH, Frankfurt am Main, Germany).

Table S–II. General PCR program used for the amplification of fragments and linearized vectors.

Step	Temp. [°C]	Duration	Cycle
Initial denaturation	98	3 min	
Denaturation	98	10 s	
Annealing	Primer dep. (-0.5 °C per cycle)	30 s	10x
Elongation	72	30 s/kbp	
Denaturation	98	10 s	
Annealing	Primer dep.	30 s	17x
Elongation	72	30 s/kbp	
Final elongation	72	5 min	

Table S–III. Primers used for cloning.

Primer #	Sequence (5'-3')	Comment / Construct
1	TAATACGACTCACTATAGGG	T7 promotor
2	GCTAGTTATTGCTCAGCGG	T7 terminator
3	GCCAAGCAGATCGCCGTGCACTCTGATGACTGGCGAATAC	TFD-EE E154H for
4	GTATTCGCCAGTCATCAGAGTGCACGGCGATCTGCTTGGC	TFD-EE E154H rev
5	AGCCTTGATGGAAACGACTTAAACATC	TFD-EH T87E short for
6	CCACCATTGAACTTAGCCTTGATGGAAACGACTTAAACATC	TFD-EH T87E long for
7	CCCCGAACTTCAGCGCT	TFD-EH T87E short rev
8	AAGTTCAATGGTGGCCCCGAACTTCAGCG	TFD-EH T87E long rev
9	AACGGCGGCGGTGGTGATGTGGACGAAATGTTAAAGCAG	Take out Ferredoxin domain from TFDs long for
10	GTGGACGAAATGTTAAAGCAG	Take out Ferredoxin domain from TFDs short for
11	AACGATGAGGATATCACCACCC	Take out Ferredoxin domain from TFDs short rev
12	ATCACCACCGCCGCCGTTAACGATGAGGATATCACCACCC	Take out Ferredoxin domain from TFDs long rev

The purified products were hybridized according to the SLIM protocol in **Table S–IV**. After hybridization, chemically competent *E. coli* DH10ß cells were transformed by heat shock: following the addition of the assembly mixture, cells were incubated on ice for 30 min, followed by 60-75 s heat shock at 42 °C, addition of 500 µL LB medium or SOC medium (20 g/L tryptone, 5 g/L yeast extract, 584 mg/L sodium chloride, 186 mg/L potassium chloride, 2 g/L magnesium chloride hexahydrate, 1204 mg/L magnesium sulfate, 3.6 g/L glucose) and incubation for 1 h at 37 °C while shaking at 650 rpm. Afterward, transformed cells were cultivated overnight on kanamycin-containing LB agar plates at 37 °C. The successful assembly of the desired vector was tested by colony PCR and sequences were verified by Sanger sequencing (GENEWIZ Germany GmbH, Leipzig, Germany).

Table S–IV. General program used for the hybridization of the linearized vectors following SLIM.

Step	Temp. [°C]	Duration [min]
Initial Denaturation	98	3
Annealing	65	5
Hybridization step 1	30	40
Annealing	65	5
Hybridization step 2	30	40

S1.2–DNA and protein sequences of all constructs

1. Starting scaffold: TFD-EE (E31, E154)

PDB code: 6ZV9

N-His6x-TEV (cleavable) (pET-M11 vector)

Full-length protein: M_W = 21880.26 Da, ε_{280} = 19480 $M^{-1}cm^{-1}$

TEV-cleaved protein: M_W = 18881.96 Da, ε_{280} = 16500 $M^{-1}cm^{-1}$

ATGAAACATCACCATCACCATCAC**CCCATGAGCGATTACGACATCCCCACTACT**GAGAATCTTTATTTTCA
GGGC**GCCATGGGT**GATATTTTGATTGTGTGGGCTAAGGACGTGGATGAAATGCTGAAACAAGTTGAGATTT
TACGCCGTCTTGGAGCGAAACAAATTGCAGTA**GAA**TCCTCGGATTGGCGTATCTTACAGGAAGCACTGAAA
AAGGGTGGTGATATCCTCATCGTTAACGGCGGCGGAATGACAATTACTTTTCGCGGGGATGACCTTGAAGC
GTTACTGAAAGCGGCTATCGAGATGATCAAACAAGCGCTGAAGTTCGGGGCCACCATTACCCTTAGCCTTG
ATGGAAACGACTTAAACATCAATATCACAGGTGTCCCGGAACAGGTACGCAAGGAATTGGCCAAAGAAGCA
GAGCGTTTAGCTAAAGAATTTGGAATTACGGTCACGCGCACTGGGGGTGGTGATGTGGACGAAATGTTAAA
GCAGGTAGAAATTCTTCGTCGCTTAGGGGCAAAACAAATCGCTGTC**GAA**AGTGATGACTGGCGCATTCTCC
AGGAAGCCCTCAAAAAGGGC**TAA**

MKHHHHHH**PMSDYDIPTTENLYFQGAMG**DILIVWAKDVDEMLKQVEILRRLGAKQIAV**E**SSDWRILQEALK
KGGDILIVNGGGMTITFRGDDLEALLKAAIEMIKQALKFGATITLSLDGNDLNINITGVPEQVRKELAKEA
ERLAKEFGITVTRTGGGDVDEMLKQVEILRRLGAKQIAV**E**SDDWRILQEALKKG*****

2. TFD-QQ (Q31, Q154)

N-His6x-TEV (cleavable) (pET-M11 vector)

Full-length protein: M_W = 21878.29 Da, ε_{280} = 19480 $M^{-1}cm^{-1}$

TEV-cleaved protein: M_W = 18879.99 Da, ε_{280} = 16500 $M^{-1}cm^{-1}$

ATGAAACATCACCATCACCATCAC**CCCATGAGCGATTACGACATCCCCACTACT**GAGAATCTTTATTTTCA
GGGC**GCCATGGGT**GATATTTTGATTGTGTGGGCTAAGGACGTGGATGAAATGCTGAAACAAGTTGAGATTT
TACGCCGTCTTGGAGCGAAACAAATTGCAGTA**CAA**TCCTCGGATTGGCGTATCTTACAGGAAGCACTGAAA
AAGGGTGGTGATATCCTCATCGTTAACGGCGGCGGAATGACAATTACTTTTCGCGGGGATGACCTTGAAGC
GTTACTGAAAGCGGCTATCGAGATGATCAAACAAGCGCTGAAGTTCGGGGCCACCATTACCCTTAGCCTTG
ATGGAAACGACTTAAACATCAATATCACAGGTGTCCCGGAACAGGTACGCAAGGAATTGGCCAAAGAAGCA
GAGCGTTTAGCTAAAGAATTTGGAATTACGGTCACGCGCACTGGGGGTGGTGATGTGGACGAAATGTTAAA
GCAGGTAGAAATTCTTCGTCGCTTAGGGGCAAAACAAATCGCTGTC**CAA**AGTGATGACTGGCGCATTCTCC
AGGAAGCCCTCAAAAAGGGC**TAA**

MKHHHHHH**PMSDYDIPTTENLYFQGAMG**DILIVWAKDVDEMLKQVEILRRLGAKQIAV**Q**SSDWRILQEALK
KGGDILIVNGGGMTITFRGDDLEALLKAAIEMIKQALKFGATITLSLDGNDLNINITGVPEQVRKELAKEA
ERLAKEFGITVTRTGGGDVDEMLKQVEILRRLGAKQIAV**Q**SDDWRILQEALKKG*****

3. TFD-EH (E31, H154)

PDB codes: 9QUC, 9QUD, 9QUI

N-His6x-TEV (cleavable) (pET-M11 vector)

Full-length protein: M_W = 21888.29 Da, ε_{280} = 19480 $M^{-1}cm^{-1}$

TEV-cleaved protein: M_W = 18889.99 Da, ε_{280} = 16500 $M^{-1}cm^{-1}$

ATGAAACATCACCATCACCATCAC**CCCATGAGCGATTACGACATCCCCACTACT**GAGAATCTTTATTTTCA
GGGC**GCCATGGGT**GATATTTTGATTGTGTGGGCTAAGGACGTGGATGAAATGCTGAAACAAGTTGAGATTT
TACGCCGTCTTGGAGCGAAACAAATTGCAGTA**GAA**TCCTCGGATTGGCGTATCTTACAGGAAGCACTGAAA
AAGGGTGGTGATATCCTCATCGTTAACGGCGGCGGAATGACAATTACTTTTCGCGGGGATGACCTTGAAGC
GTTACTGAAAGCGGCTATCGAGATGATCAAACAAGCGCTGAAGTTCGGGGCCACCATTACCCTTAGCCTTG
ATGGAAACGACTTAAACATCAATATCACAGGTGTCCCGGAACAGGTACGCAAGGAATTGGCCAAAGAAGCA
GAGCGTTTAGCTAAAGAATTTGGAATTACGGTCACGCGCACTGGGGGTGGTGATGTGGACGAAATGTTAAA
GCAGGTAGAAATTCTTCGTCGCTTAGGGGCAAAACAAATCGCTGTC**CAC**AGTGATGACTGGCGCATTCTCC
AGGAAGCCCTCAAAAAGGGC**TAA**

MKHHHHHH**PMSDYDIPTTENLYFQGAMG**DILIVWAKDVDEMLKQVEILRRLGAKQIAV**E**SSDWRILQEALK
KGGDILIVNGGGMTITFRGDDLEALLKAAIEMIKQALKFGATITLSLDGNDLNINITGVPEQVRKELAKEA
ERLAKEFGITVTRTGGGDVDEMLKQVEILRRLGAKQIAV**H**SDDWRILQEALKKG*

4. TFD-EH T87E (E31, E87, H154)

PDB codes: 9QUL, 9QUO

N-His6x-TEV (cleavable) (pET-M11 vector)

Full-length protein: M_W = 21916.30 Da, ε_{280} = 19480 $M^{-1}cm^{-1}$

TEV-cleaved protein: M_W = 18918.00 Da, ε_{280} = 16500 $M^{-1}cm^{-1}$

ATGAAACATCACCATCACCATCAC**CCCATGAGCGATTACGACATCCCCACTACT**GAGAATCTTTATTTTCA
GGGC**GCCATGGGT**GATATTTTGATTGTGTGGGCTAAGGACGTGGATGAAATGCTGAAACAAGTTGAGATTT
TACGCCGTCTTGGAGCGAAACAAATTGCAGTA**GAA**TCCTCGGATTGGCGTATCTTACAGGAAGCACTGAAA
AAGGGTGGTGATATCCTCATCGTTAACGGCGGCGGAATGACAATTACTTTTCGCGGGGATGACCTTGAAGC
GTTACTGAAAGCGGCTATCGAGATGATCAAACAAGCGCTGAAGTTCGGGGCCACCATT**GAA**CTTAGCCTTG
ATGGAAACGACTTAAACATCAATATCACAGGTGTCCCGGAACAGGTACGCAAGGAATTGGCCAAAGAAGCA
GAGCGTTTAGCTAAAGAATTTGGAATTACGGTCACGCGCACTGGGGGTGGTGATGTGGACGAAATGTTAAA
GCAGGTAGAAATTCTTCGTCGCTTAGGGGCAAAACAAATCGCTGTC**CAC**AGTGATGACTGGCGCATTCTCC
AGGAAGCCCTCAAAAAGGGC**TAA**

MKHHHHHH**PMSDYDIPTTENLYFQGAMG**DILIVWAKDVDEMLKQVEILRRLGAKQIAV**E**SSDWRILQEALK
KGGDILIVNGGGMTITFRGDDLEALLKAAIEMIKQALKFGATI**E**LSLDGNDLNINITGVPEQVRKELAKEA
ERLAKEFGITVTRTGGGDVDEMLKQVEILRRLGAKQIAV**H**SDDWRILQEALKKG*

5. TIM-barrel of TFD-EE (TIM-EE) (E31, E154)

N-His6x-TEV (cleavable) (pET-M11 vector)

Full-length protein: M_W = 13750.84 Da, ε_{280} = 19480 $M^{-1}cm^{-1}$

TEV-cleaved protein: M_W = 10752.54 Da, ε_{280} = 16500 $M^{-1}cm^{-1}$

ATGAAACATCACCATCACCATCAC**CCCATGAGCGATTACGACATCCCCACTACT**GAGAATCTTTATTTTCA
GGGC**GCCATGGGT**GATATTTTGATTGTGTGGGCTAAGGACGTGGATGAAATGCTGAAACAAGTTGAGATTT
TACGCCGTCTTGGAGCGAAACAAATTGCAGTA**GAA**TCCTCGGATTGGCGTATCTTACAGGAAGCACTGAAA
AAGGGTGGTGATATCCTCATCGTTAACGGCGGCGGGGGTGGTGATGTGGACGAAATGTTAAAGCAGGTAGA
AATTCTTCGTCGCTTAGGGGCAAAACAAATCGCTGTC**GAA**AGTGATGACTGGCGCATTCTCCAGGAAGCCC
TCAAAAAGGGC**TAA**

MKHHHHHH**PMSDYDIPTTENLYFQGAMG**DILIVWAKDVDEMLKQVEILRRLGAKQIAV**E**SSDWRILQEALK
KGGDILIVNGGGGDVDEMLKQVEILRRLGAKQIAV**E**SDDWRILQEALKKG*

6. TFD-EE MPNN (E31, E154)

PDB code: 9QUP

N-His6x-TEV (cleavable) (pET29b(+) vector)

Full-length protein: M_W = 21629.96 Da, ε_{280} = 19480 $M^{-1}cm^{-1}$

TEV-cleaved protein: M_W = 18631.66 Da, ε_{280} = 16500 $M^{-1}cm^{-1}$

ATGAAACACCATCATCACCACCAT**CCGATGTCCGATTATGACATTCCTACCACG**GAAAATCTGTACTTTCA
AGGG**GCTATGGGCATG**ATGACTTTTATAGTTTGGGCTCTGAATAAAGATGAGATGCTCAAAAATATAGAAG
CTCTGCGCAAAGCCGGTGCAAAAAATATAGCAGTA**GAA**TCAGGAGATTTTGACATACTTCGCGCCGCGATT
GAAGCGGGCGTCGAAACCATCGTCGTTTCTGGGGGAGGTCTCACCATCGTCTTCACTGGCGCTGACCGGGC
CGCGCTGCGGCGCGCTGCAAAACGTCTCCTGGATGCGGCCTTGGAACTGGGTGCTGTCGTAACAGTAGCTT
TAGATGGCGATGCACTTCGCGTTCGTATTACGGGCGTTCCAGAGCAAGATCTGGAGAGATTGAGAGCTCTG
GCCCGTGAACTGGCTGCGGAATTTGGTATTGAGGTGGAGGTTAGAGGGGGTGGAACCCCCGAACGCGCATT
GCGTGAAATTCAGGAATTGCGCGAACTCGGAGCCAAAAATATTTGGGTG**GAG**TCGGCAAACGTAGATTGGC
TGCTTAAACTTCTGAAACTGAGC**TGA**

MKHHHHHH**PMSDYDIPTTENLYFQGAMGM**MTFIVWALNKDEMLKNIEALRKAGAKNIAV**E**SGDFDILRAAI
EAGVETIVVSGGGLTIVFTGADRAALRRAAKRLLDAALELGAVVTVALDGDALRVRITGVPEQDLERLRAL
ARELAAEFGIEVEVRGGGTPERALREIQELRELGAKNIWV**E**SANVDWLLKLLKLS*

S2–CRYSTALLOGRAPHIC DATA

S2.1–Crystallographic parameters

Table S–V. Crystallization conditions

Structure	Preparation method	Incubation temperature [°C]	Protein to reservoir ratio [µL/µL]	Protein solution	Reservoir solution
Metal-free TFD-EH PDB code: 9QUC	Hanging drop	4	1.0/1.0	10 mg/mL protein 1 mM $CuCl_2$ 25 mM HEPES pH 7.0	20 % (w/v) PEG 3350 0.1 M Potassium citrate
TFD-EH+Cu^{II} PDB code: 9QUD	Hanging drop	20	1.0/1.0	9 mg/mL protein 2 mM $CuCl_2$ 25 mM HEPES pH 7.0	12 % (w/v) PEG 6000 0.05 M imidazole pH 7.0
TFD-EH+Ni^{II} PDB code: 9QUI	Hanging drop	20	1.0/1.0	9 mg/mL protein 2 mM $NiCl_2$ 25 mM HEPES pH 7.0	12 % (w/v) PEG 6000 0.05 M imidazole pH 8.5
TFD-EH T87E+Zn^{II} PDB code: 9QUL	Hanging drop	20	1.0/1.0	9 mg/mL protein 2 mm $ZnCl_2$ 25 mM HEPES pH 7.0	16 % (w/v) PEG 6000 0.05 M imidazole pH 7.0
TFD-EH T87E+Co^{II} PDB code: 9QUO	Hanging drop	20	1.0/1.0	9 mg/mL protein 2 mM $CoCl_2$ 25 mM HEPES pH 7.0	14 % (w/v) PEG 6000 0.05 M imidazole pH 7.0
TFD-EE MPNN +Tb^{III} PDB code: 9QUP	Sitting drop	20	0.2/0.1	9 mg/mL protein 250 µM $TbCl_3$ 25 mM HEPES pH 7.5 25 mM NaCl	25 % (w/v) PEG 3350 0.1 M Tris pH 8.5 0.2 M NaCl

Table S-VI Crystallographic data collection and refinement statistics of TFD-EH apo and TFD-EH:Cu^{II}

	Metal-free TFD-EH	**TFD-EH+Cu^{II}**	**TFD-EH+Cu^{II} [Cu^{II} (peak)]**
Crystal parameters			
Space group	$P3_121$	$P3_121$	$P3_121$
Cell constants (Å)	a = 78.7 b = 78.7 c = 66.3	a = 76.8 b = 76.8 c = 70.0	a = 76.8 b = 76.8 c = 70.0
Subunits / AU[a]	1	1	1
Data collection			
Beam line	X06SA, SLS	X06SA, SLS	X06SA, SLS
Wavelength (Å)	1.0	1.0	1.377
Resolution range (Å)[b]	30-1.60 (1.70-1.60)	30-1.95 (2.05-1.95)	30-2.05 (2.15-2.05)
No. observations	192292	73117	123991
No. unique reflections[c]	31409	17755	28979[#]
Completeness (%)[b]	99.1 (99.4)	99.7 (100.0)	99.8 (100.0)
R_{merge} (%)[b, d]	3.9 (58.7)	3.3 (68.7)	3.5 (56.8)
I/σ(I)[b]	20.3 (2.7)	19.0 (2.0)	19.7 (2.7)
Refinement (REFMAC5)			
Resolution range (Å)	30-1.60	30-1.95	
No. refl. working set	29824	16856	
No. refl. test set	1569	887	
No. non hydrogen	1514	1423	
No. of ligand atoms (Cu)	-	1	
Solvent (H_2O, ions, glycerol, PEG, citrate, imidazole)	194	111	
R_{work} / R_{free} (%)[e]	15.7/18.4	16.6/21.8	
r.m.s.d. bond (Å) / (°)[f]	0.003/1.1	0.003/1.1	
Average B-factor ($Å^2$)	32.2	47.8	
Ramachandran plot (%)[g]	97.6/2.4/0	98.8/1.2/0	
PDB-ID	9QUC	9QUD	

[a] Asymmetric unit

[b] The values in parentheses for resolution range, completeness, R_{merge} and I/σ (I) correspond to the highest resolution shell

[c] Data reduction was carried out with XDS and from a single crystal. [#]Friedel pairs were treated as individual reflections

[d] $R_{merge}(I) = \Sigma_{hkl}\Sigma_j \mid I(hkl)_j - \langle I(hkl)\rangle \mid / \Sigma_{hkl}\, \Sigma_j\, I(hkl)_j$, where $I(hkl)_j$ is the j^{th} measurement of the intensity of reflection hkl and $\langle I(hkl)\rangle$ is the average intensity

[e] $R = \Sigma_{hkl} \mid |F_{obs}| - |F_{calc}| \mid / \Sigma_{hkl} |F_{obs}|$, where R_{free} is calculated without a sigma cut off for a randomly chosen 5% of reflections, which were not used for structure refinement, and R_{work} is calculated for the remaining reflections

[f] Deviations from ideal bond lengths/angles

[g] Number of residues in favored region / allowed region / outlier region

Table S–VII Crystallographic data collection and refinement statistics of TFD-EH:Ni^{II}

	TFD-EH+Ni^{II}	**TFD-EH+Ni^{II} [Ni^{II} (peak)]**
Crystal parameters		
Space group	$P3_121$	$P3_121$
Cell constants (Å)	a = 76.7 b = 76.7 c = 71.2	a = 76.7 b = 76.7 c = 71.2
Subunits / AU[a]	1	1
Data collection		
Beam line	P13, PETRA III, DESY	P13, PETRA III, DESY
Wavelength (Å)	976	1.485
Resolution range (Å)[b]	30-2.10 (2.20-2.10)	30-2.20 (2.30-2.20)
No. observations	72915	132264
No. unique reflections[c]	13957	23819[#]
Completeness (%)[b]	96.1 (98.7)	99.9 (99.9)
R_{merge} (%)[b, d]	4.2 (71.0)	7.3 (65.4)
I/σ(I)[b]	19.4 (2.3)	14.2 (3.8)
Refinement (REFMAC5)		
Resolution range (Å)	30-2.10	
No. refl. working set	13253	
No. refl. test set	697	
No. non hydrogen	1352	
No. of ligand atoms (Ni, Co)	1	
Solvent (H_2O, ions, glycerol, PEG, citrate, imidazole)	40	
R_{work} / R_{free} (%)[e]	18.5/22.3	
r.m.s.d. bond (Å) / (°)[f]	0.003/1.2	
Average B-factor (Å^2)	60.8	
Ramachandran Plot (%)[g]	98.8/1.2/0	
PDB-ID	9QUI	

[a] Asymmetric unit

[b] The values in parentheses for resolution range, completeness, R_{merge} and I/σ (I) correspond to the highest resolution shell

[c] Data reduction was carried out with XDS and from a single crystal. [#]Friedel pairs were treated as individual reflections

[d] $R_{merge}(I) = \Sigma_{hkl}\Sigma_j | I(hkl)_j - \langle I(hkl)\rangle | / \Sigma_{hkl} \Sigma_j I(hkl)_j$, where $I(hkl)_j$ is the j^{th} measurement of the intensity of reflection hkl and $\langle I(hkl)\rangle$ is the average intensity

[e] $R = \Sigma_{hkl} | |F_{obs}| - |F_{calc}| | / \Sigma_{hkl} |F_{obs}|$, where R_{free} is calculated without a sigma cut off for a randomly chosen 5% of reflections, which were not used for structure refinement, and R_{work} is calculated for the remaining reflections

[f] Deviations from ideal bond lengths/angles

[g] Number of residues in favored region / allowed region / outlier region

Table S–VIII Crystallographic data collection and refinement statistics of TFD-EH T87E:Zn^{II} and TFD-EH T87E:Co^{II}

	TFD-EH T87E+Zn^{II}	**TFD-EH T87E+Zn^{II} [Zn^{II} (peak)]**	**TFD-EH T87E+Co^{II}**	**TFD-EH T87E+Co^{II} [Co^{II} (peak)]**
Crystal parameters				
Space group	$P3_121$	$P3_121$	$P3_121$	$P3_121$
Cell constants (Å)	a = 76.2 b = 76.2 c = 70.3	a = 76.2 b = 76.2 c = 70.3	a = 76.4 b = 76.4 c = 70.8	a = 76.4 b = 76.4 c = 70.8
Subunits / AU[a]	1	1	1	1
Data collection				
Beam line	P13, PETRA III, DESY	P13, PETRA III, DESY	P13, PETRA III, DESY	P13, PETRA III, DESY
Wavelength (Å)	976	1.282	976	1.604
Resolution range (Å)[b]	30-1.90 (2.00-1.90)	30-1.85 (1.95-1.85)	30-1.95 (2.05-1.95)	30-1.95 (2.05-1.95)
No. observations	52145	168701	70361	159543
No. unique reflections[c]	18249[#]	38905[#]	17125	33337[#]
Completeness (%)[b]	96.0 (98.2)	99.8 (100.0)	96.2 (98.6)	99.0 (99.7)
R_{merge} (%)[b, d]	5.8 (66.5)	7.7 (56.2)	5.3 (51.3)	7.3 (64.7)
I/σ(I)[b]	9.3 (1.6)	10.8 (2.5)	13.9 (2.7)	12.2 (2.3)
Refinement (REFMAC5)				
Resolution range (Å)	30-1.90		30-1.95	
No. refl. working set	17330		16265	
No. refl. test set	912		856	
No. non hydrogen	1381		1392	
No. of ligand atoms (Zn, Co)	1		1	
Solvent (H_2O, ions, glycerol, PEG, citrate, imidazole)	76		78	
R_{work} / R_{free} (%)[e]	18.1/21.9		19.0/21.9	
r.m.s.d. bond (Å) / (°)[f]	0.003/1.1		0.003/1.2	
Average B-factor ($Å^2$)	44.1		40.6	
Ramachandran Plot (%)[g]	98.2/1.8/0		99.4/0.6/0	
PDB-ID	9QUL		9QUO	

[a] Asymmetric unit
[b] The values in parentheses for resolution range, completeness, R_{merge} and I/σ (I) correspond to the highest resolution shell
[c] Data reduction was carried out with XDS and from a single crystal. [#]Friedel pairs were treated as individual reflections

[d] $R_{merge}(I) = \Sigma_{hkl}\Sigma_j \mid I(hkl)_j - \langle I(hkl)\rangle \mid / \Sigma_{hkl}\, \Sigma_j\, I(hkl)_j$, where $I(hkl)_j$ is the j^{th} measurement of the intensity of reflection hkl and $\langle I(hkl)\rangle$ is the average intensity

[e] $R = \Sigma_{hkl} \mid |F_{obs}| - |F_{calc}| \mid / \Sigma_{hkl} |F_{obs}|$, where R_{free} is calculated without a sigma cut off for a randomly chosen 5% of reflections, which were not used for structure refinement, and R_{work} is calculated for the remaining reflections

[f] Deviations from ideal bond lengths/angles

[g] Number of residues in favored region / allowed region / outlier region

Table S–IX Crystallographic data collection and refinement statistics of TFD-EE MPNN:Tb^{III}

	TFD-EE MPNN:Tb^{III}
Crystal parameters	
Space group	$P2_12_12_1$
Cell constants (Å)	a = 42.98 b = 66.44 c = 94.37
Subunits / AU[a]	2
Data collection	
Beam line	P13, PETRA III, DESY
Wavelength (Å)	976
Resolution range (Å)[b]	30-1.95 (2.05-1.95)
No. observations	109376
No. unique reflections[c]	20002
Completeness (%)[b]	98.2 (96.1)
Rmerge (%)[b, d]	9.7 (78.4)
I/σ(I)[b]	16.29 (2.51)
Refinement (REFMAC5)	
Resolution range (Å)	30-1.95
No. refl. working set	18996
No. refl. test set	999
No. non hydrogen	26543
No. of ligand atoms (Zn, Co)	1
Solvent (H_2O, ions, glycerol, PEG, citrate, imidazole)	55
R_{work} / R_{free} (%)[e]	19.6/22.6
r.m.s.d. bond (Å) / (°)[f]	0.002/1.144
Average B-factor ($Å^2$)	36.9
Ramachandran Plot (%)[g]	100/0/0
PDB-ID	9QUP

[a] Asymmetric unit

[b] The values in parentheses for resolution range, completeness, R_{merge} and I/σ (I) correspond to the highest resolution shell

[c] Data reduction was carried out with XDS and from a single crystal. #Friedel pairs were treated as individual reflections

[d] $R_{merge}(I) = \Sigma_{hkl}\Sigma_j | I(hkl)_j - \langle I(hkl)\rangle | / \Sigma_{hkl} \Sigma_j I(hkl)_j$, where $I(hkl)_j$ is the j^{th} measurement of the intensity of reflection hkl and $\langle I(hkl)\rangle$ is the average intensity

[e] $R = \Sigma_{hkl} | |F_{obs}| - |F_{calc}| | / \Sigma_{hkl} |F_{obs}|$, where R_{free} is calculated without a sigma cut off for a randomly chosen 5% of reflections, which were not used for structure refinement, and R_{work} is calculated for the remaining reflections

[f] Deviations from ideal bond lengths/angles

[g] Number of residues in favored region / allowed region / outlier region

S2.2–Crystal structures of TFD-EE, TFD-EH, and TFD-EH T87E

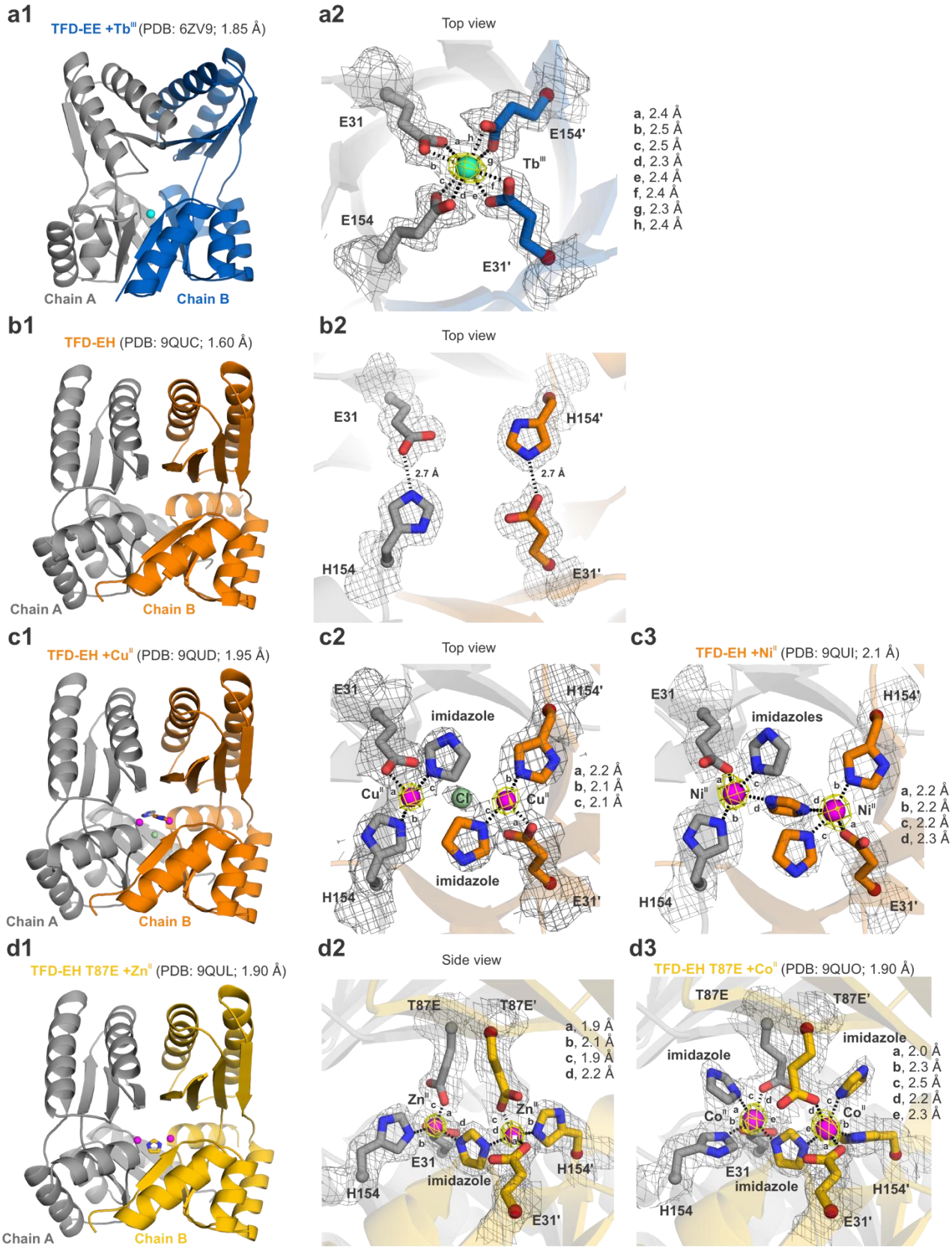

Figure S1. Crystal structures of TFD-EE, TFD-EH, and TFD-EH T87E with metal ions.

The protein backbones are shown in cartoon representation, with metal ions as spheres and coordination bonds highlighted as dotted lines. **a1, a2,** TFD-EE bound to Tb^{III}, PDB code 6ZV9, showing eight coordination bonds. 2Fo-Fc electron density is shown as a grey mesh contoured at 1.0 σ. Anomalous electron density is shown as a yellow mesh at 20.0 σ. **b1, b2,** TFD-EH, in the metal-free state, the binding residues are stabilized via hydrogen bonds, PDB code 9QUC. TFD-EH complexed with Cu^{II} adopts a square planar geometry (with an unsatisfied charge), PDB code 9QUD. TFD-EH complexed with Ni^{II} exhibits tetrahedral coordination, PDB code 9QUI. 2Fo-Fc electron density is shown as a gray mesh contoured at 1.0 σ. Anomalous electron density is shown as a yellow mesh at 4.0 σ for Cu^{II} and 5.0 σ for Ni^{II}. **c1, c2, c3**, TFD-EH T87E coordinated to Zn^{II} and Co^{II}, PDB codes 9QUL and 9QUO, respectively. 2Fo-Fc electron density is shown as a gray mesh contoured at 1.0 σ. Anomalous electron density is shown as a yellow mesh at 10.0 σ for both metals.

S3–BIOPHYSICAL CHARACTERIZATION OF THE SCAFFOLDS

S3.1–Circular dichroism spectra of TFD variants

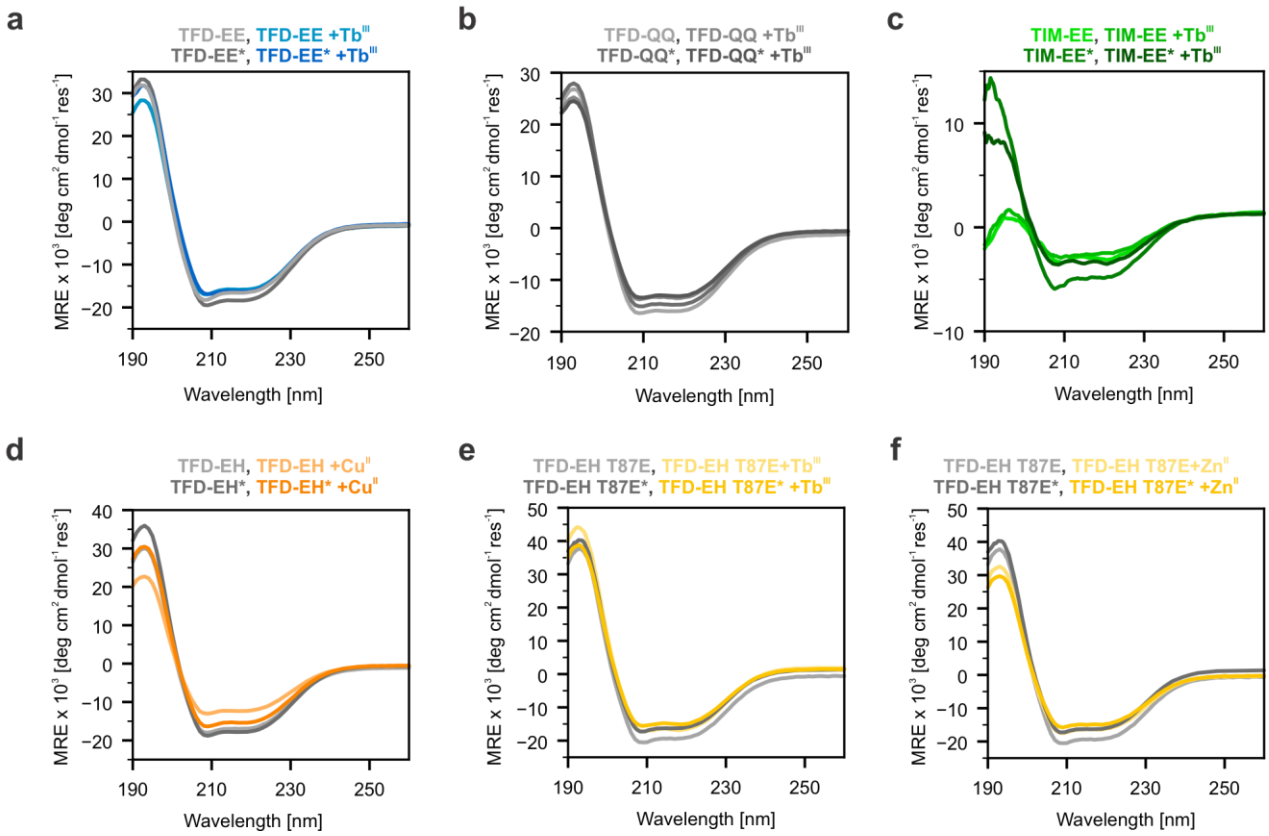

Figure S2. Circular dichroism spectra of TFD-EE, TFD-EH, and TFD-EH T87E.

a, TFD-EE (metal-free and with Tb^{III}). When the metal-free TFD-EE is at room temperature, it exhibits a shifted signal minimum of 205 nm. In all other conditions, the minimum remains at 208–209 nm. **b,** TFD-QQ (metal-free and with Tb^{III}). TFD-QQ displays the same spectral shape at both room temperature and 40 °C, regardless of metal binding or heating treatment. **c,** TIM-EE (metal-free and with Tb^{III}). TIM-EE shows improved CD signal intensity after heating, which is further enhanced by metal binding. The most unfolded condition is observed at room temperature, and metal alone does not provide a clear stabilizing effect. **d,** TFD-EH (metal-free and with Cu^{II}). TFD-EH retains the same overall spectral shape at both temperatures, with or without metal addition. **e**,**f,** TFD-EH T87E (metal-free and with Tb^{III} and Zn^{II}). Similar to TFD-EH, this variant also maintains consistent spectral features at room temperature and 40 °C, regardless of metal binding.

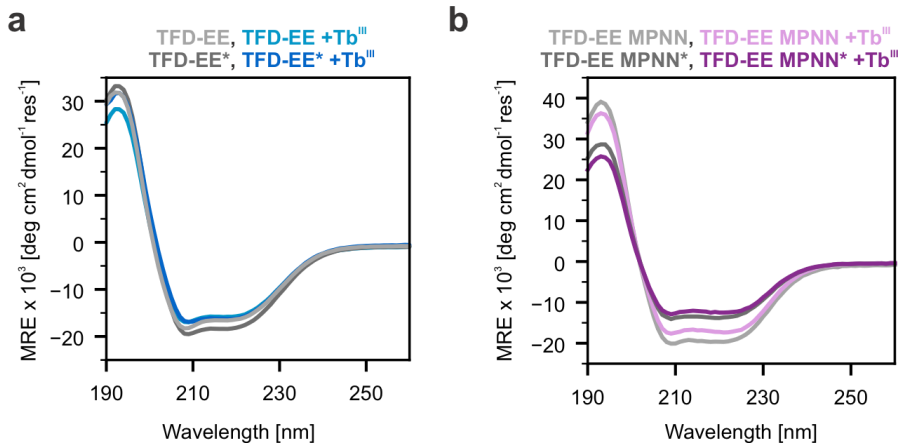

Figure S3. Circular dichroism spectra of the TFD-EE and TFD-EE MPNN.

a, TFD-EE (metal-free and with Tb^{III}). When the metal-free TFD-EE is at room temperature, it exhibits a shifted signal minimum of 205 nm. In all other conditions, the minimum remains at 208–209 nm. **b,** TFD-EE MPNN (metal-free in gray and with Tb^{III} in purple). This variant displays a similar spectral shape at both room temperature and 40 °C, regardless of metal binding or heating treatment. The signal is decreased after heating treatment, but the protein still shows a conserved secondary structure.

S3.2–SEC-SLS data of TFD variants

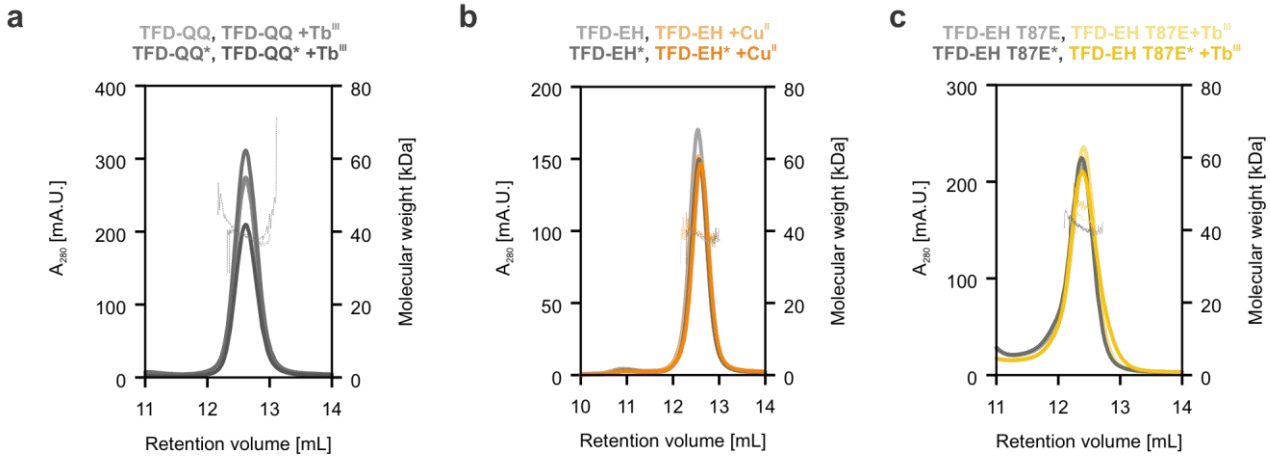

Figure S4. SEC-SLS profiles of TFD-QQ, TFD-EH, and TFD-EH T87E.

a, TFD-QQ (metal-free and with Tb^{III}). A single peak is observed under all conditions and temperatures, indicating a stable dimeric species with no significantly higher-order oligomers. **b,** TFD-EH (metal-free and with Cu^{II}). Like TFD-QQ, TFD-EH displays only one peak in every condition, consistent with a single dimeric species. **c,** TFD-EH T87E (metal-free and with Tb^{III}). This variant also shows a single peak across all conditions and temperatures, again suggesting a stable dimer with negligible higher-order oligomer formation.

S4–PROTEIN NUCLEAR MAGNETIC RESONANCE SPECTROSCOPY

S4.1–Backbone Assignment of TFD-EE

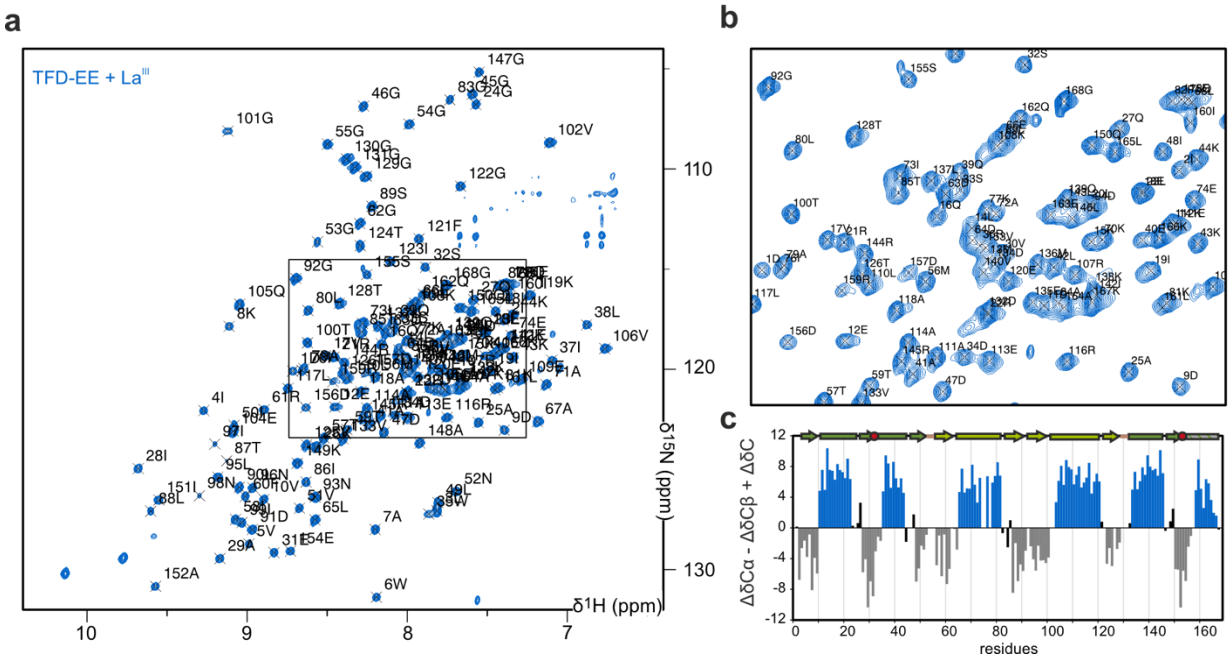


```
TFD-EE          DILIVWAKDVDEMLKQVEILRRLGAKQIAVESSDWRILQEALKKGGDILIVNGGGMTITF  60
TFD-EE          RGDDLEALLKAAIEMIKQALKFGATITLSLDGNDLNINITGVPEQVRKELAKEAERLAKE 120
TFD-EE          FGITVTRTGGGDVDEMLKQVEILRRLGAKQIAVESDDWRILQEALKKG              168

Assigned residues: 165/168
```

Figure S5. Backbone resonances assignment of La^{III}-bound TFD-EE by NMR.

a, ^{1}H-^{15}N HSQC spectrum of La^{III}-bound triple-labeled TFD-EE with peak assignment labeled on the spectrum and a zoom on the central, overlapped region shown in **b**. **c,** The differences of chemical shifts of the backbone carbon atoms compared to their reference values in random coil regions indicate the α-helical propensity (positive values, in blue) and β-strand propensity (negative values, in gray) of the residue.

The spectra of La^{III}-bound triple-labeled TFD-EE (protein concentration= 2 mM) were recorded at 800 MHz and 25 °C in NMR buffer (25 mM HEPES pH 7.0, 25 mM NaCl), using 12 scans and 200 increments. Backbone resonances were assigned using HNCACB, CBCA(CO)NH, HNCO, and HN(CA)CO spectra. Residues assigned are highlighted in yellow along the sequence, resulting in 98% coverage. The chemical shifts have been deposited in the BMRB (entry 53123).

S4.2–Backbone Assignment of TFD-EH

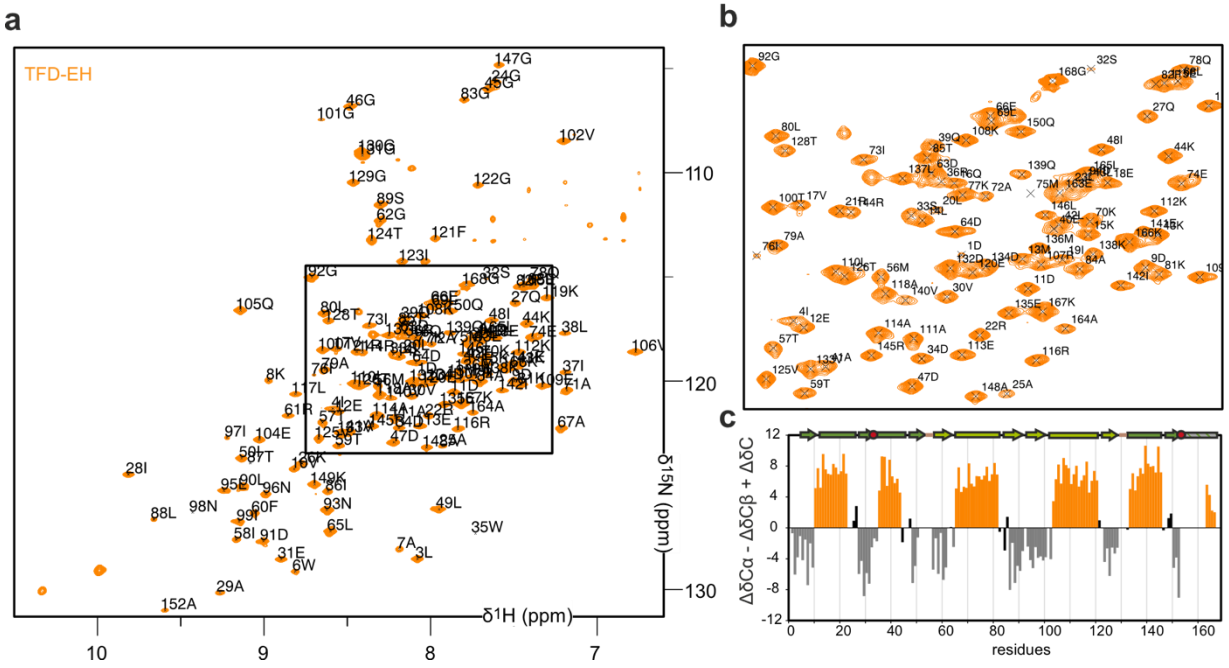


```
TFD-EH          DILIVWAKDVDEMLKQVEILRRLGAKQIAVESSDWRILQEALKKGGDILIVNGGGMTITF 60
TFD-EH          RGDDLEALLKAAIEMIKQALKFGATITLSLDGNDLNINITGVPEQVRKELAKEAERLAKE 120
TFD-EH          FGITVTRTGGGDVDEMLKQVEILRRLGAKQIAVHSDDWRILQEALKKG             168

Assigned residues: 150/168
```

Figure S6. Backbone resonances assignment of metal-free TFD-EH by NMR.

a, ^{1}H-^{15}N HSQC spectrum of triple-labeled TFD-EH with peak assignment labeled on the spectrum and a zoom on the central, overlapped region shown in **b**. **c,** The differences of chemical shifts of the backbone carbon atoms compared to their reference values in random coil regions indicate the alpha helical propensity (positive values, in orange) and beta strand propensity (negative values, in gray) of the residue.

A spectrum of 1 mM triple-labeled TFD-EH was recorded at 800 MHz and 25 °C in NMR buffer (25 mM HEPES pH 7.0, 25 mM NaCl), using 12 scans and 200 increments. Backbone resonances were assigned using HNCACB and CBCA(CO)NH experiments, with HNCO, and HN(CA)CO spectra as validation. Residues assigned are highlighted in yellow along the sequence, resulting in 89% coverage. The chemical shifts have been deposited in the BMRB (entry 53124).

S4.3–Metal titrations to TFD-QQ

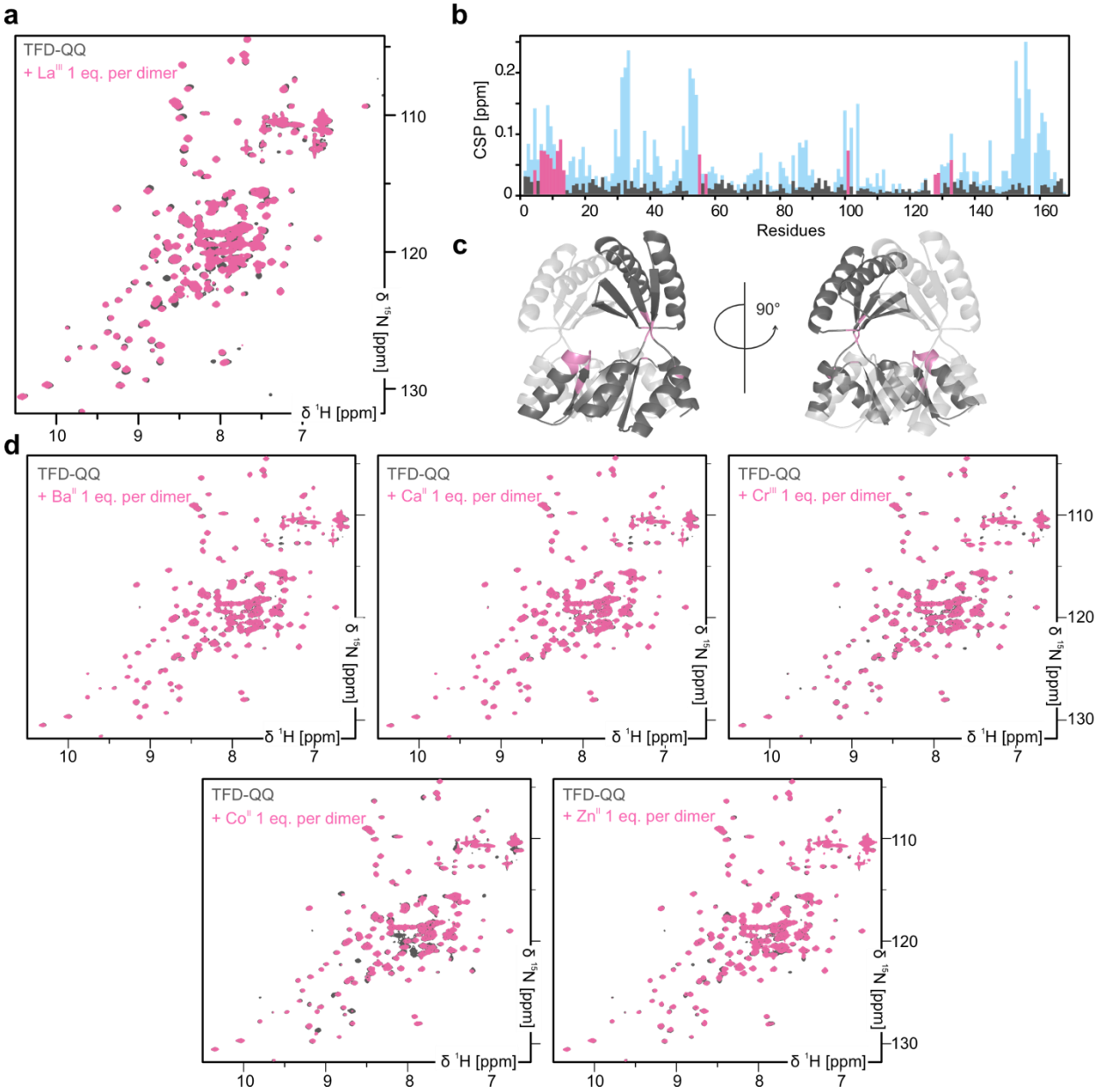

Figure S7. NMR characterization of TFD-QQ, the metal-binding "knockout" variant of TFD-EE, in the presence of different metal ions.

a, ^{1}H-^{15}N HSQC spectrum of TFD-QQ with La^{III} at a 1:1 ratio. TFD-QQ was designed to lack a functional metal-binding site, and the limited chemical shift changes suggest minimal interaction with La^{III}. **b,** Residue-specific chemical shift perturbations (CSPs) plotted in gray for TFD-QQ with vs. without La^{III}, highlighting in pink the highest values observed in residues far from the binding site. The CSP for TFD-EE with vs. without La^{III,} is shown in blue for comparison to highlight the difference in scale for specific vs. nonspecific metal binding. **c,** The localized changes in TFD-QQ are consistent with nonspecific surface binding as shown in the cartoon representations of the protein. **d,** Additional ^{1}H-^{15}N HSQC spectra of TFD-QQ in the presence of Ba^{II}, Ca^{II}, Co^{II}, Cr^{III}, and Zn^{II}, each showing similarly small CSPs. Notably, the disappearance of some shifts in the presence of cobalt was expected as a paramagnetic effect of the metal ion. Together, these results confirm that TFD-QQ does not bind metals specifically in the active site, although some surface interactions may occur.

S4.4–Metal titrations to TFD-EH and TFD-EH T87E

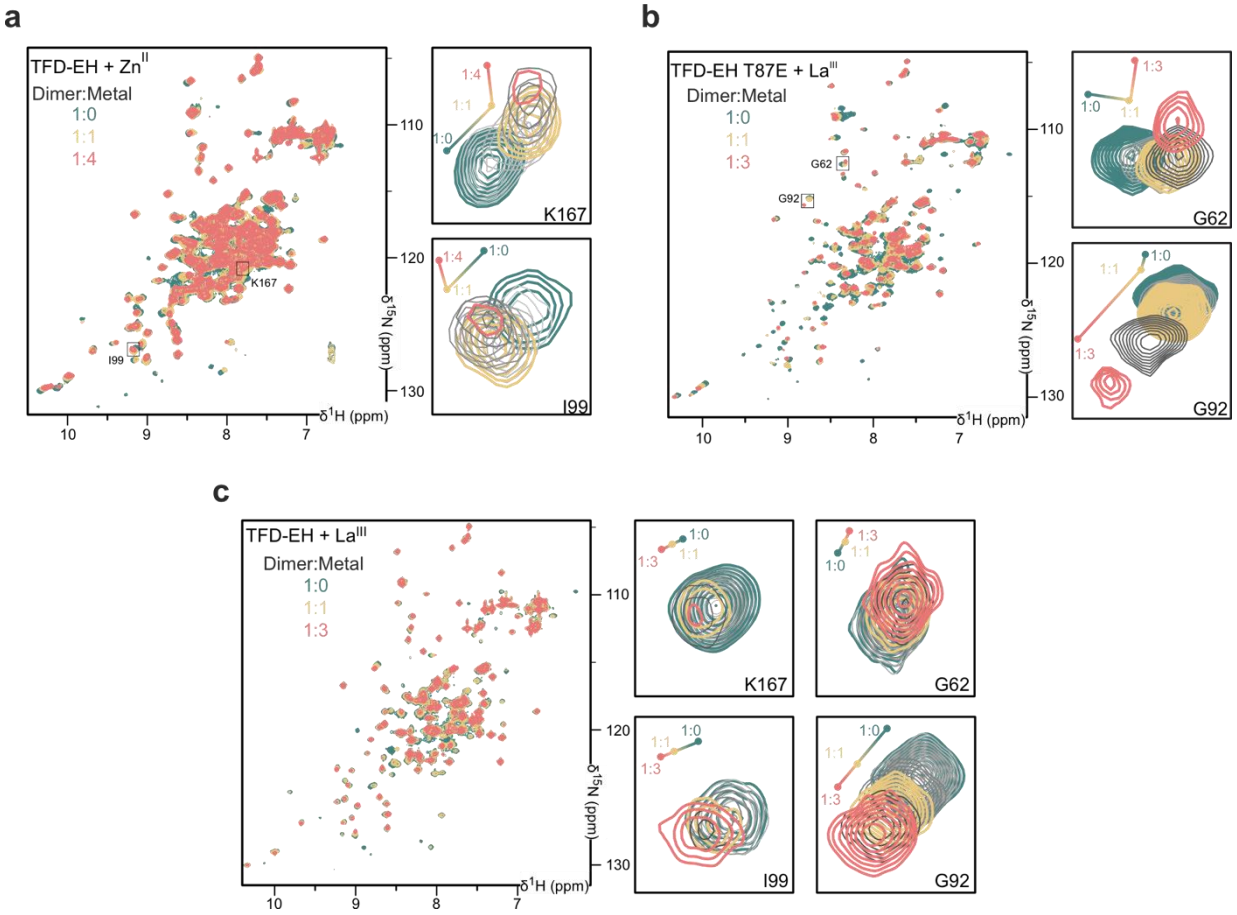

Figure S8. NMR titrations to observe metal binding to TFD-EH and TFD-EH T87E

a, ^{1}H-^{15}N HSQC spectra of TFD-EH titrated with Zn^{II} at increasing molar ratios of protein dimer to metal (0, 1, or 4 metal ions added per dimer). Residues K167 and I99 are highlighted, showing characteristic chemical shift changes in two directions, indicative of the binding of two metal ions per protein dimer. **b,** ^{1}H-^{15}N HSQC spectra of TFD-EH T87E with La^{III} at molar ratios 1:0, 1:1, and 1:3. G62 and G92 peaks are highlighted, showing the characteristic shifts that indicate binding of two metals to the protein dimer. **c,** ^{1}H-^{15}N HSQC spectra of TFD-EH titrated with La^{III} at molar ratios 1:0, 1:1, and 1:3. Highlighted residues (K167, I99, G62, and G92) are consistent with binding of a single La^{III} per dimer.

S4.5–NMR characterization of TIM-EE

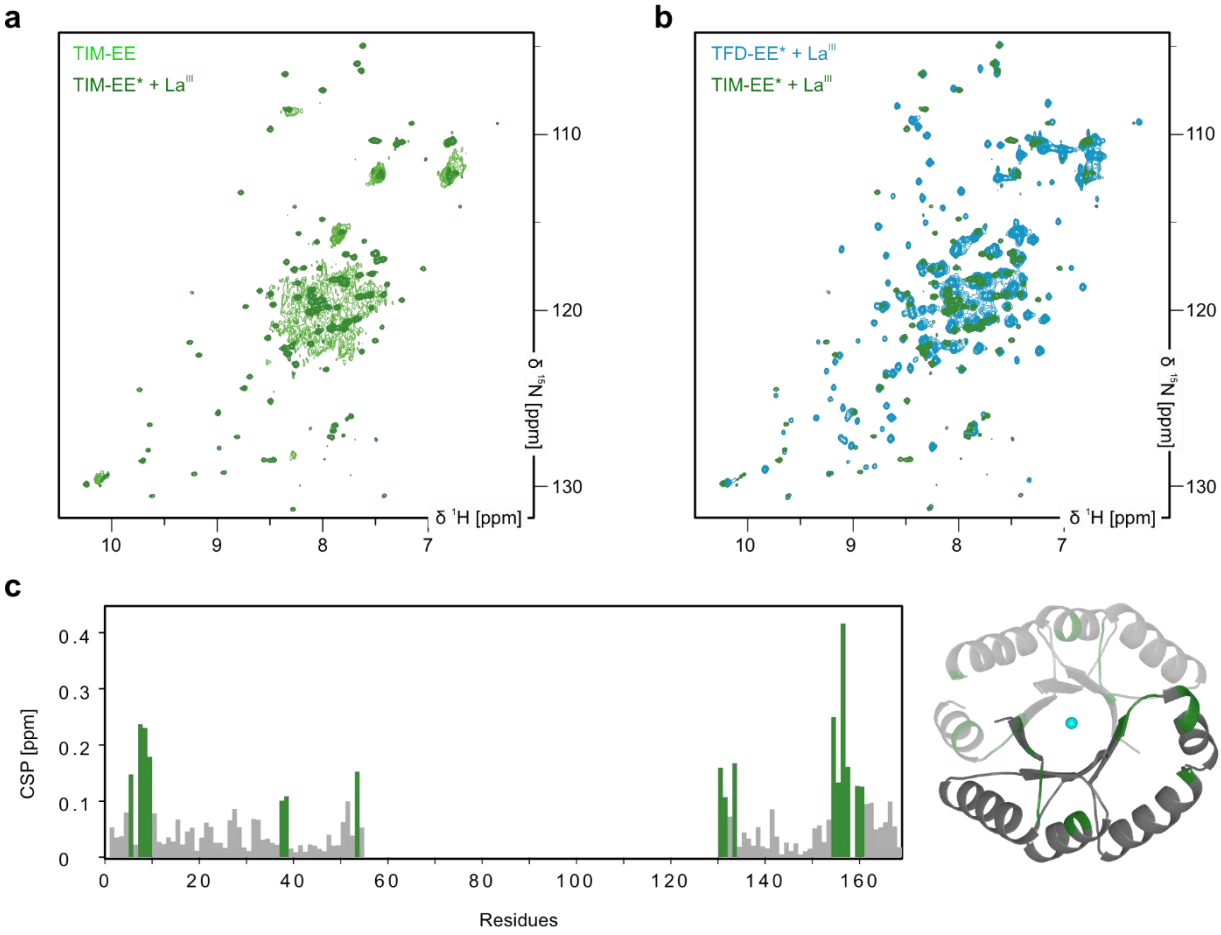

Figure S9. NMR characterization of TIM-EE, a truncated variant of TFD-EE in which the ferredoxin (FD) domain has been excised.

a, ^{1}H-^{15}N HSQC spectrum of TIM-EE in the absence (light green) and presence of La^{III} (dark green). **b**, ^{1}H-^{15}N HSQC spectra overlay of full-length TFD-EE (blue) and TIM-EE (green) after heat treatment and metal addition. **c**, Residue-specific chemical shift perturbations (CSPs) for TIM-EE + La^{III} compared to TFD-EE + La^{III}, with the missing FD region reflected in the sequence numbering. A cartoon representation of the TIM barrel is shown on the right, highlighting the most pronounced CSPs. Despite the removed FD domain, the HSQC patterns for TIM-EE and TFD-EE show a similar behavior consistent with lanthanide binding and heat treatment being essential to generate well-resolved peaks.

S4.6–Conformational ensemble analysis based on NMR pseudo-contact shifts (PCS)

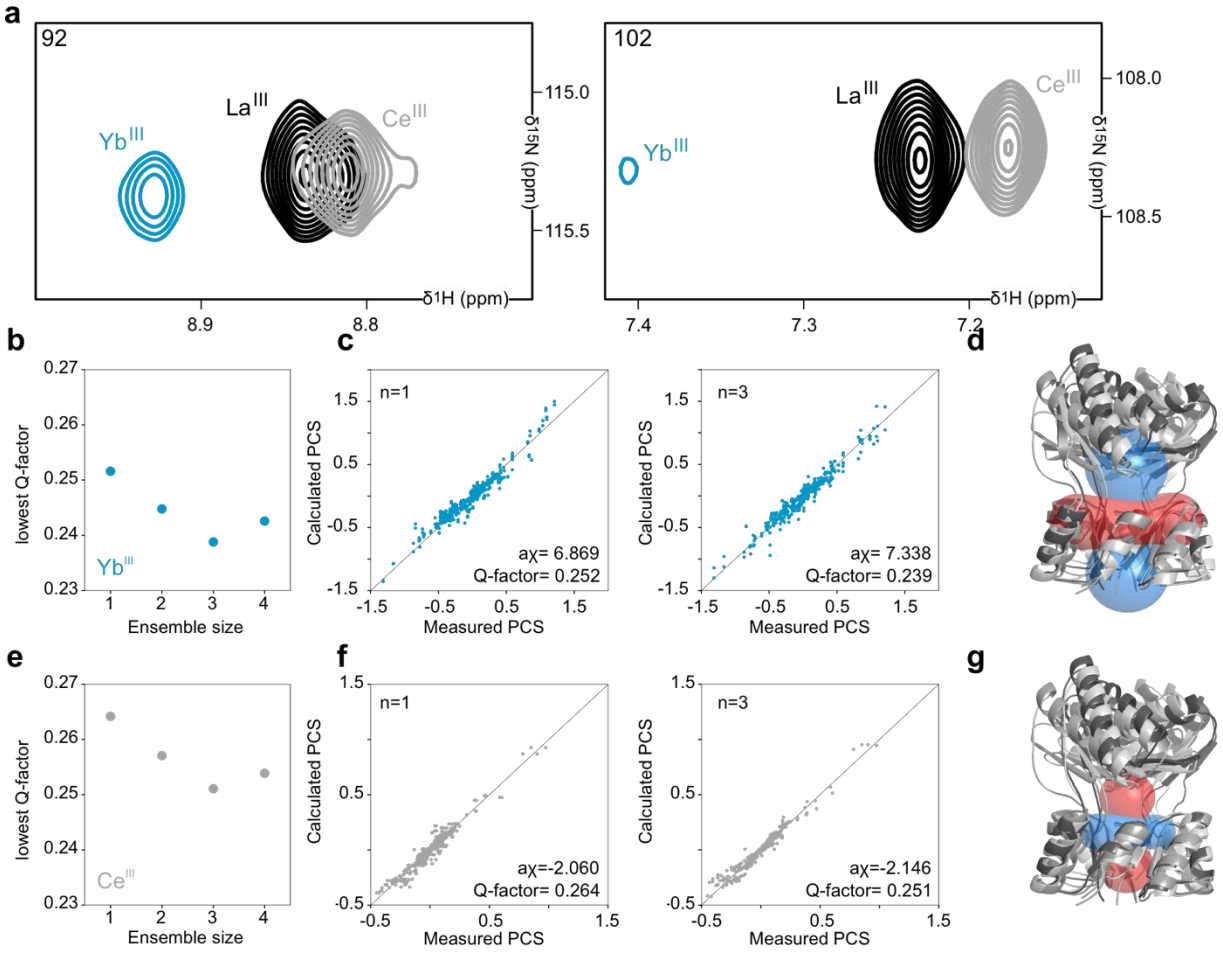

Figure S10. Ensemble analysis of PCS data from TFD-EE.

a, Extract of TFD-EE ^{1}H-^{15}N HSQC spectra for residues G92 and V102; showing the pseudo-contact shifts induced by the paramagnetic Ce^{III} and Yb^{III} compared to the diamagnetic La^{III}. **b,** Best Q-factor by ensemble size obtained for TFD-EE + Yb^{III}. **c,** Correlation between measured PCS with Yb^{III} and calculated from the model for the single best model (left) and the best ensemble (right). **d,** Visualization of the Yb^{III}-induced tensor of the best fitting ensemble with spheres indicating the 0.5ppm PCS cutoff point. **e,** Best Q-factor by ensemble size obtained for TFD-EE + Ce^{III}. **f,** Correlation between measured PCS with Ce^{III} and calculated from the model for the single best model (left) and the best ensemble (right). **g,** visualization of the Ce^{III}-induced tensor of the best fitting ensemble with spheres indicating the 0.5ppm PCS cutoff point.

S5–MOLECULAR DYNAMICS SIMULATIONS

S5.1–RMSD analysis

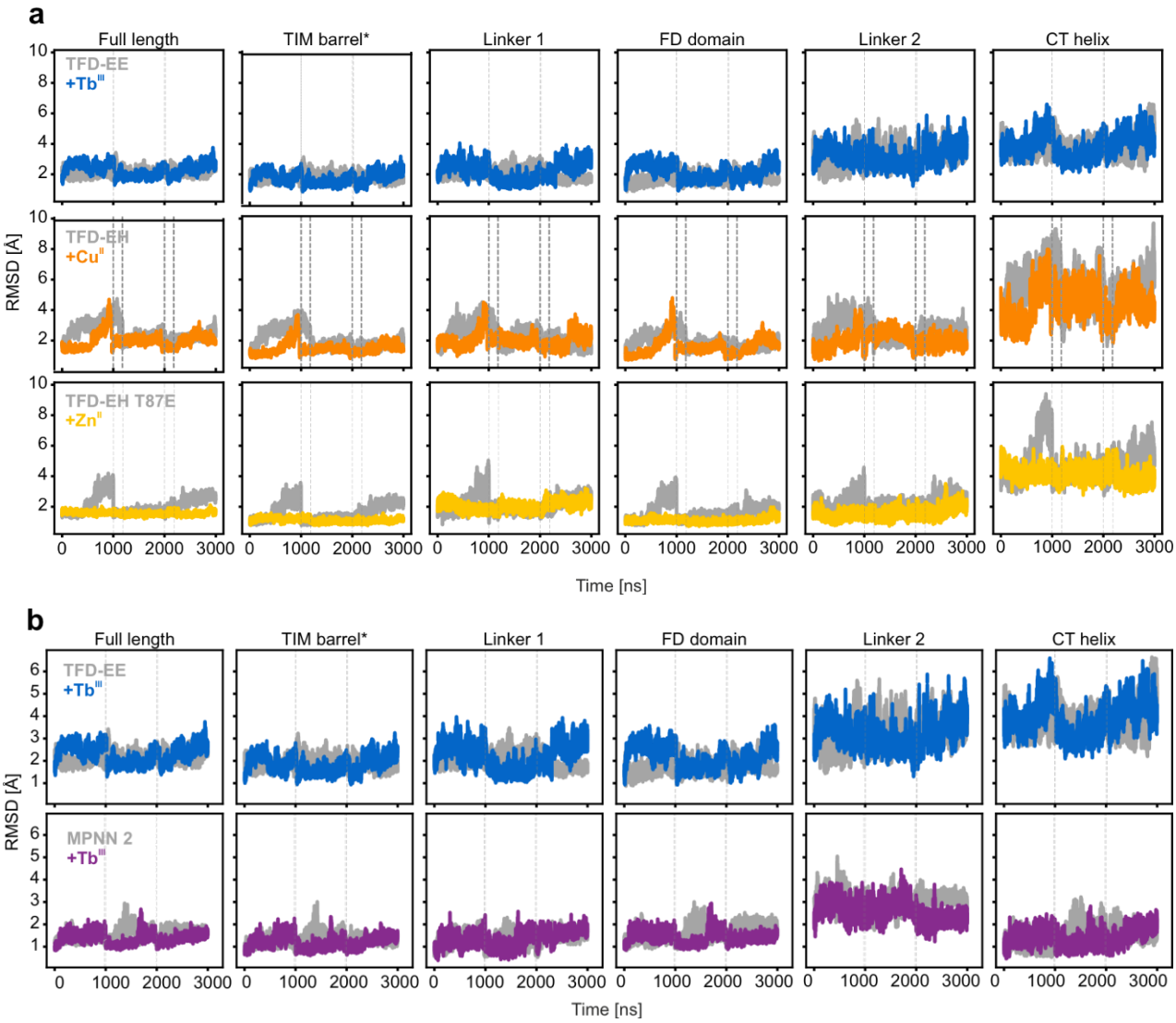

Figure S11. Time evolution of the root-mean-square deviations (RMSD) for all TFD variants.

RMSD plots of full-length proteins and of different regions in the protein defined as TIM barrel* (residues: 1-52, 132-155 (without C-terminal helix), linker 1 (residues: 53-55), FD domain (residues 56-128), linker 2 (residues: 129-131), and the C-terminal (CT) helix (residues: 156-168) are shown. **a** The metal-free time-series plots are shown in gray for all simulations, while the metal-bound states are shown in blue (TFD-EE), orange (TFD-EH), and yellow (TFD-EH T87E). **b**, The TFD-EE MPNN metal-bound state RMSDs are shown in purple and compared to the original TFD-EE in blue.

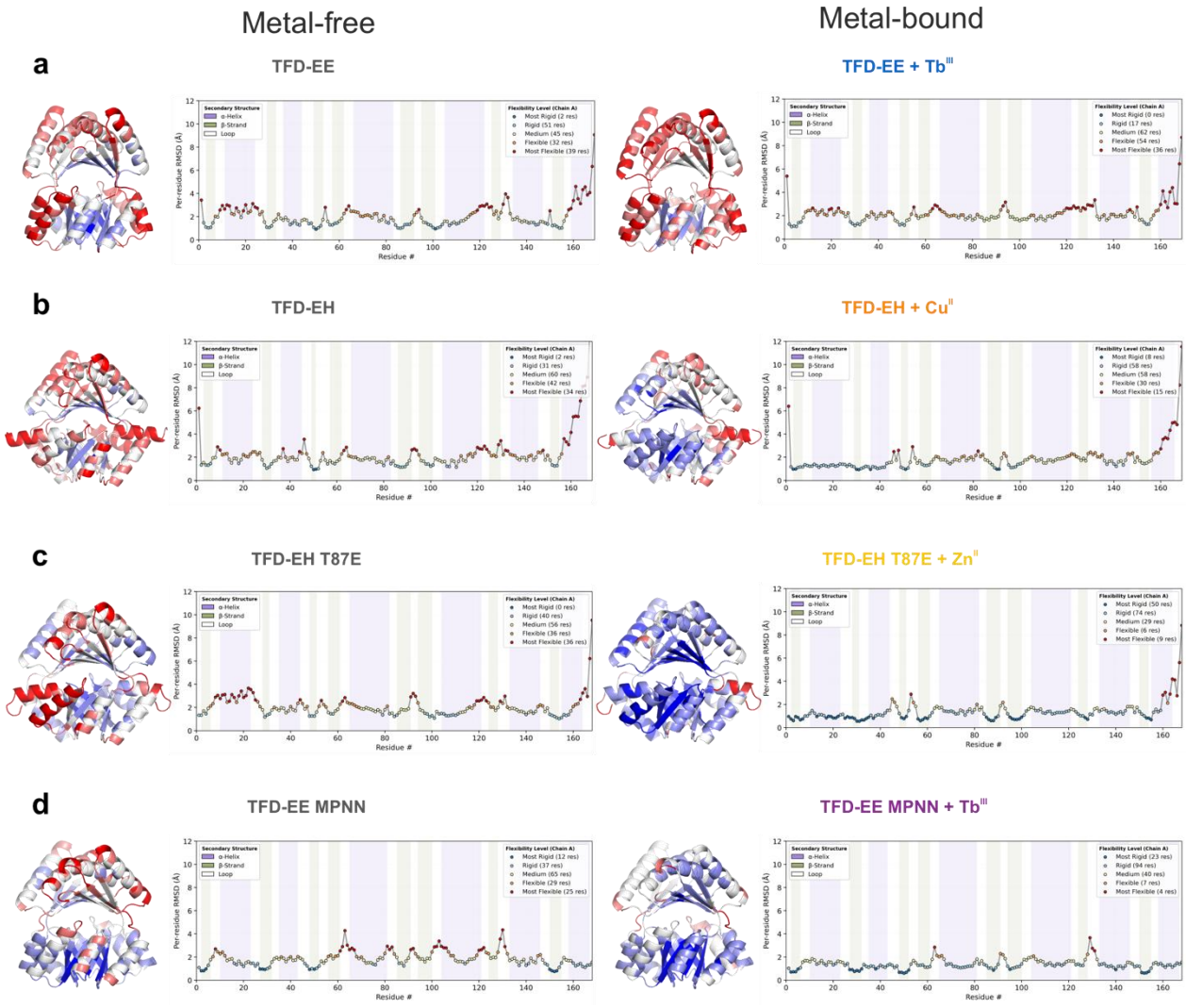

Figure S12. Per-residue RMSD calculation of all TFD variants.

Per-residue RMSD values were calculated using MDtraj [2] after superimposing the trajectory on the starting structure. Residues in the cartoon representations are color-coded on a blue-white-red scale, where blue represents rigid regions and red indicates flexible regions. The RMSD values were grouped into five levels: Level 1 (0.0-1.0 Å), Level 2 (1.0-1.5 Å), Level 3 (1.5-2.0 Å), Level 4 (2.0-2.5 Å), and Level 5 (>2.5 Å). The left side of the plot shows results for the metal-free variants, while the right side displays the corresponding metal-bound simulations. Panels a-d represent the metal-free and metal-bound comparisons for each TFD variant: TFD-EE (**a**), TFD-EH (**b**), TFD-EH T87E (**c**), and TFD-EE MPNN (**d**).

S5.2–RMSF analysis

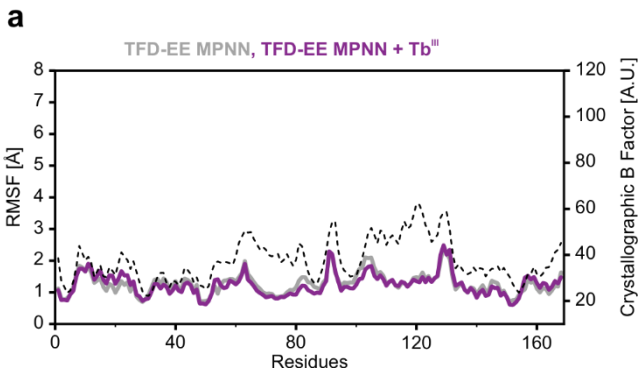

Figure S13. Root-mean-square fluctuation (RMSF) plots for TFD-EE MPNN.

RMSF of TFD-EE MPNN in the presence (purple) or absence (gray) of Tb^{III}. The x-axis indicates the residue number, while the left y-axis shows the RMSF in Å. The black dotted line represents the crystallographic B-factor for reference plotted on the right y-axis.

S5.3–Dihedral angles

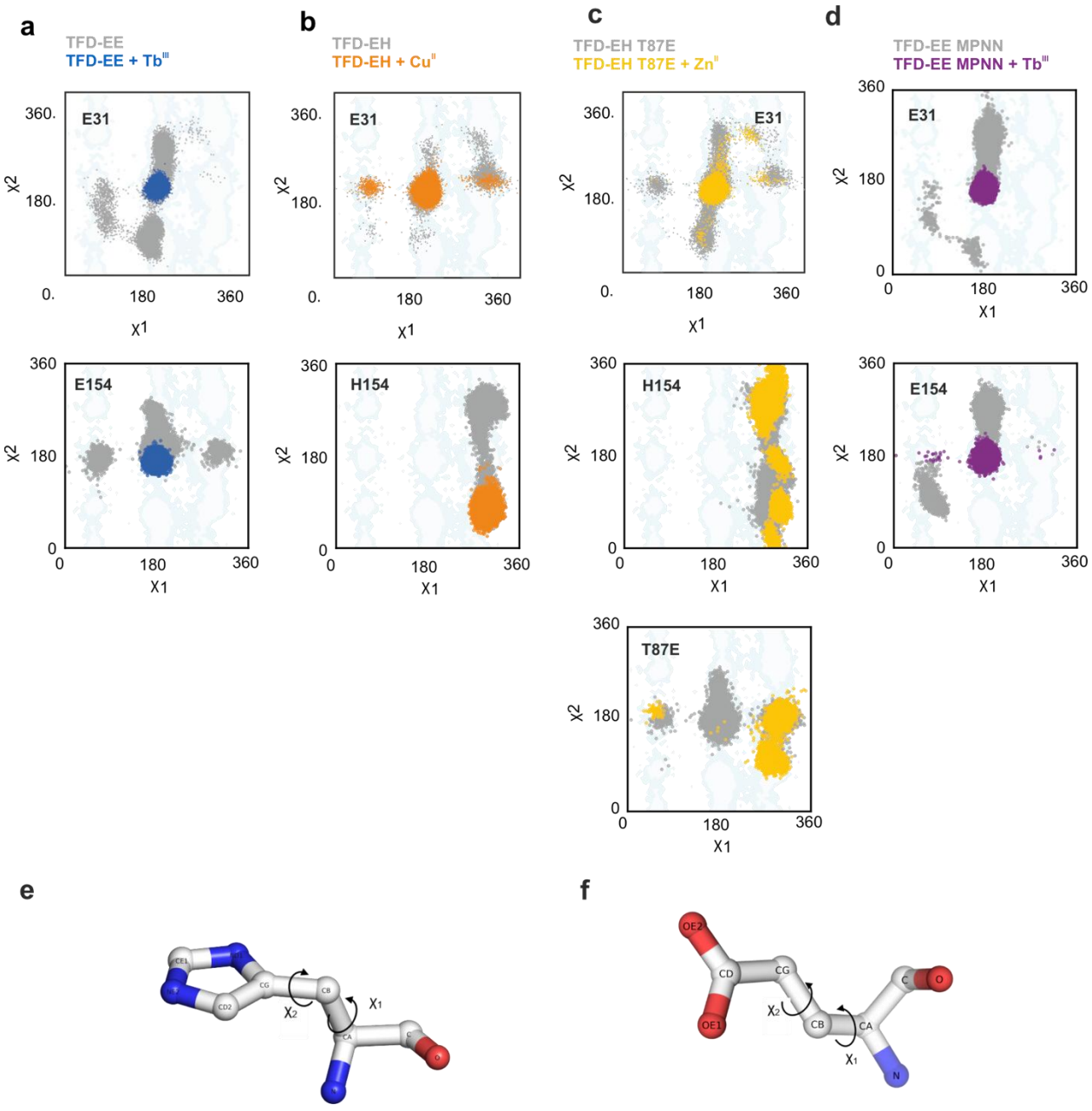

Figure S14. Side chain dihedral angle (χ1, χ2) distributions for key metal-coordinating residues in all TFD variants.

Janin plots [3-5] showing a comparison between metal-free (in gray) and metal-bound (colors) MD simulations and thus the influence of metal-binding on the side-chain flexibility of metal-coordinating residues. **a**, Dihedral angle distribution of residues E31 and E154 from TFD-EE (apo in gray, holo in blue). **b**, Dihedral angle distribution of residues E31 and H154 from TFD-EH (apo in gray, holo in orange). **c**, Dihedral angle distribution of residues E31, E87, and H154 from TFD-EH T87E (apo in gray, holo in yellow). **d**, Dihedral angle distribution of residues E31 and E154 from TFD-EE MPNN (apo in gray and holo in purple). **e**, Definition of the dihedral angle for any given glutamate and histidine (**f**).

S5.4–Principal component analysis (PCA)

a

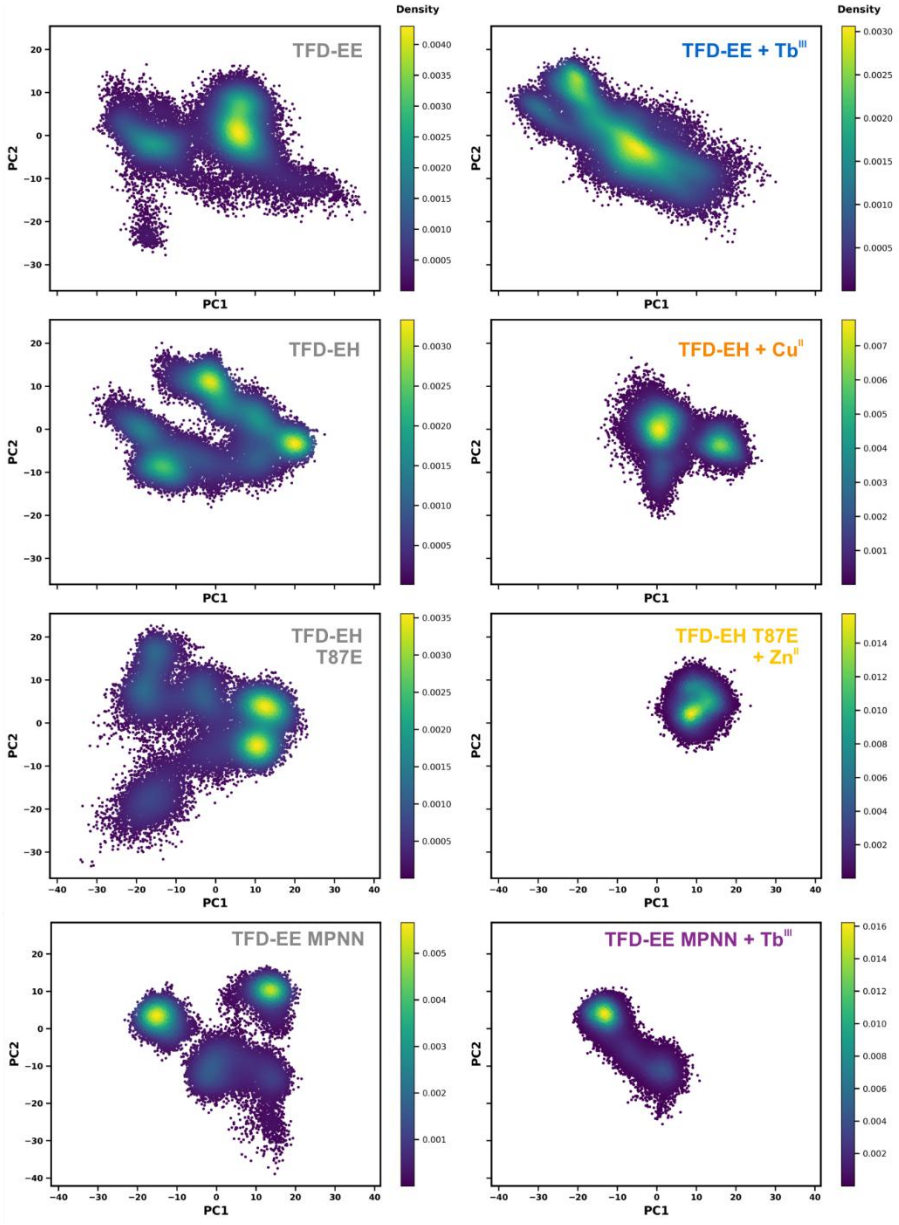

Figure S15. PCA density plots of all TFD variants.

2D density plots derived from principal component analysis (PCA) of molecular dynamics simulations for TFD variants TFD-EE, TFD-EH, TFD-EH T87E, and TFD-EE MPNN with metal-free and metal-bound simulations. Each panel represents the motion in PC1-PC2 space, with the color scale (purple to yellow) indicating increasing sampling density. The plots highlight the effect of metal binding and the difference in the conformational flexibility of each protein.

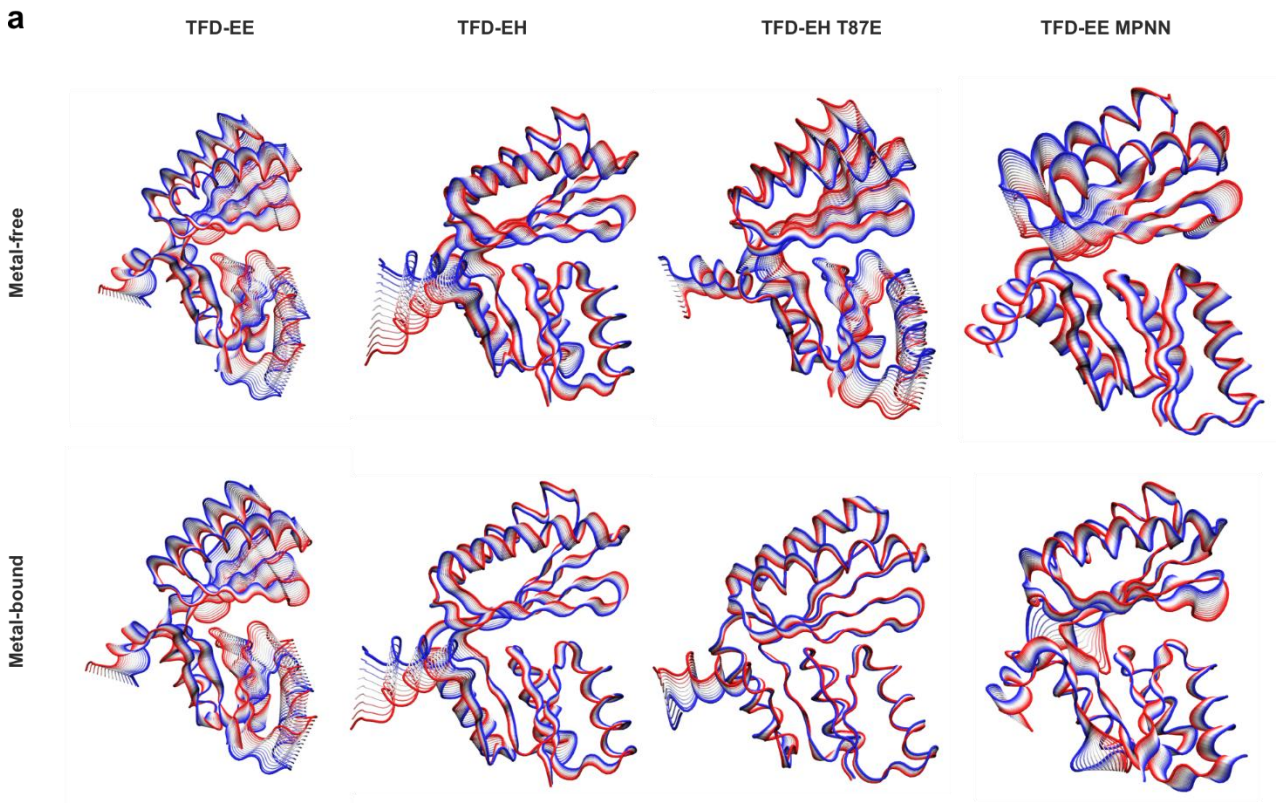

Figure S16. Representative pseudo-trajectories extracted from the principal component analysis of TFD variants.

Overlay of representative structures of TFD and MPNN variants from principal component analysis (PCA) in metal-free (top row) and metal-bound (bottom row) conditions. Each column shows one variant—TFD-EE, TFD-EH, TFD-EH T87E, and TFD-EE MPNN, color range from red (starting frame) to blue (end of frame) ribbon representations along the pseudo-trajectory defined by the first principal component (PC1). This comparison highlights how metal binding influences global domain movements and overall conformational flexibility across the different protein designs. While this figure presents static snapshots of the PCA, the corresponding motions can be viewed in **Supplementary Video S4** online.

Backbone Cα-atoms were used to perform PCA calculations in the CPPTRAJ program in AmberTools [6]. Before computing PCA modes, the rotational/translational motions were removed by fitting the trajectory to an average structure. The coordinate covariance matrix and subsequent eigenvectors (100 PC modes) and eigenvalues (weight of each PC) were calculated by diagonalizing the covariance matrix. Then, the original trajectory coordinates were projected along PCs for visualization. The holo trajectory was similarly projected using eigenvectors of the apo form to compare the variance along the PCs in apo and holo simulations. To visualize the fluctuations of the PC modes, pseudo-trajectories were generated using eigenvectors from apo and holo simulations and the min-max values (pcmin and pcmax) of the PC1 and PC2 modes.

S5.5–Interface energy analysis (ΔG)

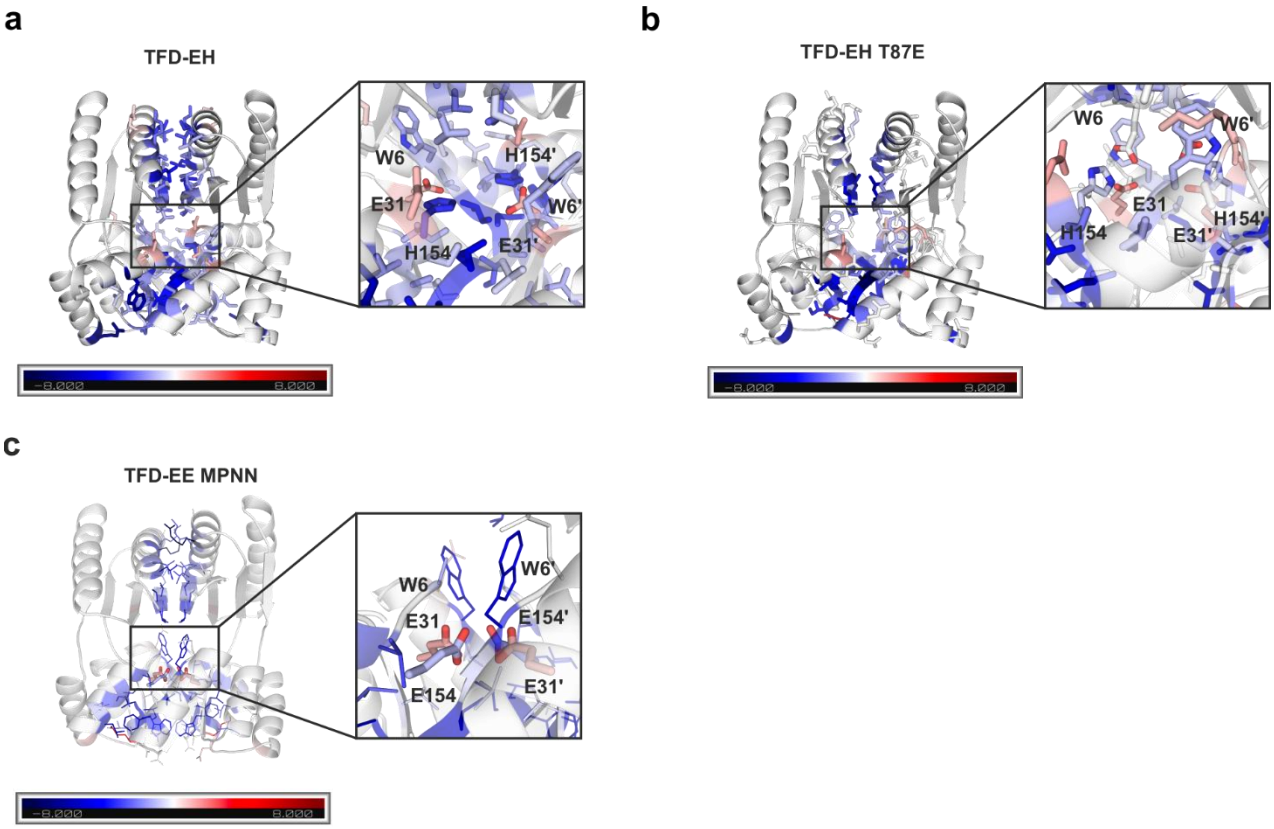

Figure S17. Analysis of the free energy contributions of dimer interface residues calculated from MD simulations.

TFD-EH (**a**), TFD-EH T87E (**b**), and TFD-EE MPNN (**c**) with their respective zoom-in views of the active site. The energy bar (blue to red) ranges from −8.000 to +8.000 A.U. The free energy of binding and contributions of each residue at the interface of the homodimers were calculated using molecular mechanics energies combined with the Poisson-Boltzmann surface area (MMPBSA) integrated in the Gromacs software (gmx_MMPBSA) [7]. The interface residues were defined by setting the cutoff to residues within 10 Å. The energy decomposition and contribution of each residue at the dimer interface were visualized in Pymol.

S6–RADICAL DIOL CLEAVAGE OF (*R*,*R*)-HYDROBENZOIN

S6.1–Reaction mechanism

a

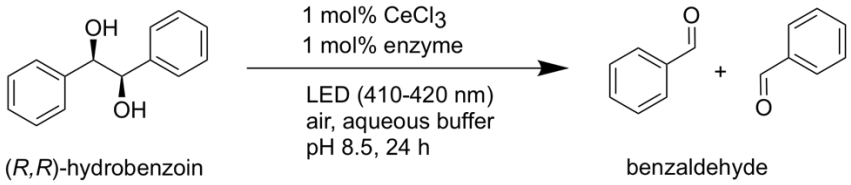

b

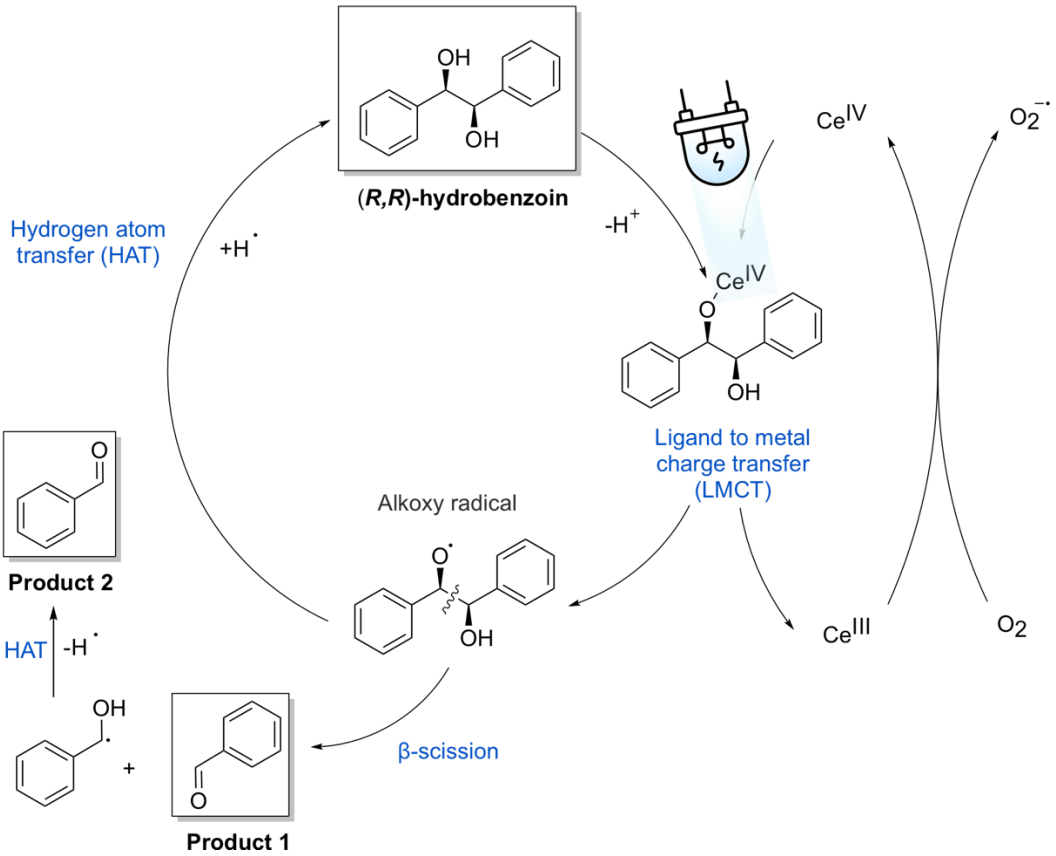

Figure S18. Photocatalytic radical cleavage of (*R*,*R*)-hydrobenzoin via cerium-bound enzyme catalysis.

a, Overall photoenzymatic reaction: (*R*,*R*)-hydrobenzoin undergoes radical C–C bond cleavage under visible light irradiation (410–420 nm) in the presence of 1 mol% $CeCl_3$ and 1 mol% TFD-EE in aqueous buffer, yielding two equivalents of benzaldehyde. **b**, Proposed mechanism: Coordination of (*R*,*R*)-hydrobenzoin to Ce^{IV} followed by photoinduced ligand-to-metal charge transfer (LMCT) generates an alkoxy radical. β-scission of the C–C bond produces one equivalent of benzaldehyde (Product 1) and a radical intermediate that undergoes hydrogen atom transfer (HAT) to produce a second equivalent of benzaldehyde (Product 2). The Ce^{III} species is reoxidized by O_2 completing the photocatalytic cycle.

S7–PROTEIN INTERACTIONS ANALYSIS

S7.1–Multiple Sequence Alignment (MSA) of the TFD-EE variants

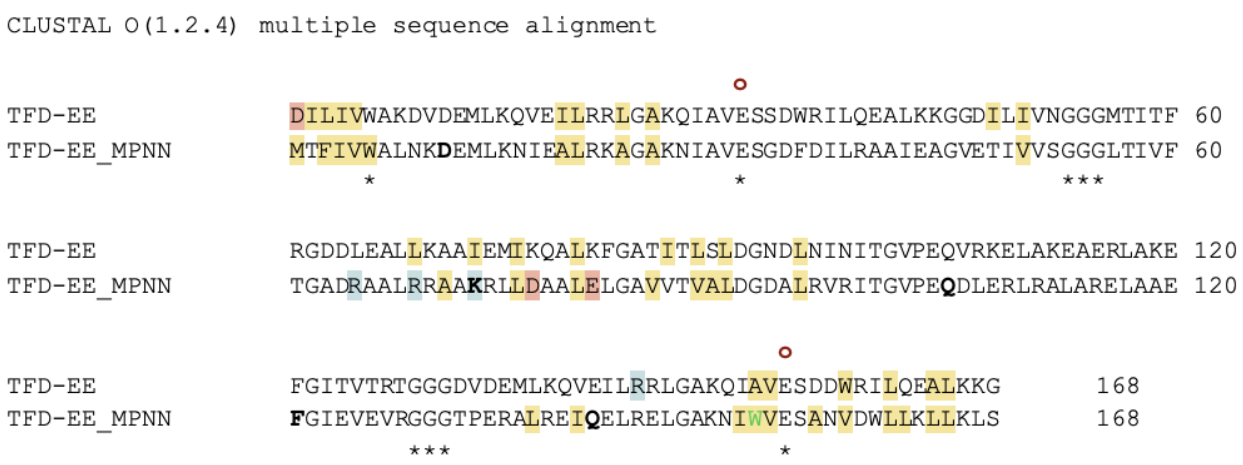

Figure S19. Multiple sequence alignment of TFD-EE and TFD-EE MPNN.

The alignment highlights nine fixed residues (*), two metal-coordinating residues (**o**), and rationally designed surface mutations (in **bold**). For TFD-EE MPNN, the rational mutations are E11D, H73K, E105Q, E121F, and E141Q. Interface interactions are indicated by colored highlights: yellow for hydrophobic clusters, cyan for positively charged residues in salt bridges, red for negatively charged residues in salt bridges, and green for π-π stacking. The total sequence length is 168 residues for both scaffolds. The MSA was performed using using CLUSTAL O(1.2.4) online tool.

S7.2–ProtInter Calculator

Table S–X. Summary from ProtInter Calculator for [TFD-EE, PDB: 6ZV9]. Intermolecular Interactions of Chain A and Chain B

cationpi (3 total):

Res1	idRes1	Ch1	Res2	idRes2	Ch2	Distance
TRP	35	A	ARG	36	A	5.79 Å
LYS	70	A	PHE	121	A	5.97 Å
TRP	158	A	ARG	159	A	5.81 Å

hbond_main_side (11 total):

Res1	idRes1	Ch1	Res2	idRes2	Ch2	Distance
MET	13	A	LEU	14	A	3.38 Å
SER	32	A	SER	33	A	3.02 Å
SER	32	A	ASP	34	A	2.94 Å
SER	33	A	ASP	34	A	3.49 Å
MET	56	A	ARG	107	A	3.60 Å
MET	75	A	LEU	110	A	3.74 Å
MET	75	A	ALA	114	A	3.76 Å
ARG	107	A	GLY	130	A	2.98 Å
MET	136	A	LEU	137	A	3.48 Å
SER	155	A	ASP	156	A	2.99 Å
SER	155	A	ASP	157	A	3.07 Å

hydrophobic (152 total):

Res1	idRes1	Ch1	Res2	idRes2	Ch2	Distance
ILE	2	A	ILE	4	A	4.22 Å
ILE	2	A	ALA	29	A	4.14 Å
ILE	2	A	ILE	48	A	4.56 Å
LEU	3	A	LEU	20	A	4.60 Å
LEU	3	A	ALA	25	A	4.81 Å
ILE	4	A	ALA	29	A	4.27 Å
ILE	4	A	ILE	50	A	4.64 Å
VAL	5	A	ALA	7	A	4.29 Å
VAL	5	A	MET	13	A	4.67 Å
VAL	5	A	VAL	17	A	4.83 Å
VAL	5	A	LEU	20	A	4.95 Å
VAL	5	A	ILE	28	A	4.27 Å
VAL	5	A	VAL	30	A	4.95 Å
ALA	7	A	MET	13	A	3.62 Å
VAL	10	A	MET	13	A	4.58 Å
VAL	10	A	LEU	14	A	4.18 Å
VAL	10	A	ILE	37	A	4.78 Å
MET	13	A	LEU	14	A	4.75 Å
MET	13	A	VAL	17	A	4.44 Å
MET	13	A	VAL	30	A	4.94 Å
MET	13	A	ILE	37	A	4.16 Å
MET	13	A	ALA	41	A	4.71 Å
VAL	17	A	ILE	28	A	4.76 Å
VAL	17	A	VAL	30	A	3.77 Å
ILE	19	A	LEU	23	A	4.49 Å
LEU	20	A	LEU	23	A	4.72 Å
LEU	20	A	ALA	25	A	4.12 Å
LEU	20	A	ILE	28	A	4.48 Å
ALA	25	A	ILE	28	A	3.75 Å
ILE	28	A	VAL	30	A	4.75 Å
ALA	29	A	ILE	48	A	3.72 Å
ALA	29	A	ILE	50	A	4.39 Å

VAL	30	A	ILE	37	A	4.19 Å
VAL	30	A	LEU	38	A	4.59 Å
VAL	30	A	ALA	41	A	3.85 Å
VAL	30	A	LEU	49	A	4.72 Å
LEU	38	A	LEU	49	A	4.81 Å
LEU	38	A	VAL	51	A	4.47 Å
LEU	38	A	LEU	143	A	4.71 Å
ALA	41	A	LEU	49	A	3.90 Å
LEU	42	A	LEU	49	A	4.70 Å
LEU	42	A	LEU	143	A	4.96 Å
LEU	42	A	LEU	146	A	3.68 Å
LEU	42	A	ALA	148	A	4.76 Å
ILE	48	A	ILE	50	A	4.25 Å
ILE	48	A	ALA	152	A	4.47 Å
LEU	49	A	LEU	143	A	4.35 Å
LEU	49	A	ALA	148	A	4.74 Å
ILE	50	A	ALA	152	A	4.36 Å
VAL	51	A	MET	136	A	4.91 Å
VAL	51	A	VAL	140	A	4.48 Å
VAL	51	A	LEU	143	A	3.79 Å
VAL	51	A	ILE	151	A	4.51 Å
VAL	51	A	VAL	153	A	4.55 Å
MET	56	A	ILE	58	A	4.47 Å
MET	56	A	ILE	99	A	4.89 Å
MET	56	A	LEU	110	A	4.07 Å
MET	56	A	ALA	111	A	3.87 Å
ILE	58	A	PHE	60	A	4.74 Å
ILE	58	A	MET	75	A	4.96 Å
ILE	58	A	ILE	97	A	4.46 Å
ILE	58	A	ILE	99	A	4.65 Å
ILE	58	A	ALA	111	A	4.58 Å
ILE	58	A	ALA	114	A	4.73 Å
ILE	58	A	VAL	125	A	4.80 Å
PHE	60	A	LEU	68	A	5.00 Å
PHE	60	A	ALA	71	A	4.51 Å
PHE	60	A	ALA	72	A	4.73 Å
PHE	60	A	MET	75	A	4.66 Å
PHE	60	A	LEU	95	A	4.53 Å
PHE	60	A	ILE	97	A	4.99 Å
PHE	60	A	ALA	114	A	4.29 Å
PHE	60	A	LEU	117	A	4.63 Å
PHE	60	A	ALA	118	A	4.44 Å
PHE	60	A	ILE	123	A	4.91 Å
PHE	60	A	VAL	125	A	4.78 Å
LEU	65	A	LEU	68	A	4.72 Å
LEU	65	A	LEU	69	A	4.35 Å
LEU	65	A	LEU	90	A	4.93 Å
ALA	67	A	PHE	121	A	4.46 Å
ALA	67	A	ILE	123	A	4.05 Å
LEU	68	A	LEU	90	A	4.81 Å
LEU	68	A	LEU	95	A	4.38 Å
LEU	68	A	ILE	123	A	4.79 Å
LEU	69	A	ILE	73	A	4.71 Å
LEU	69	A	LEU	95	A	4.93 Å
ALA	71	A	LEU	117	A	4.41 Å
ALA	71	A	PHE	121	A	4.69 Å
ALA	71	A	ILE	123	A	4.89 Å
ALA	72	A	ILE	76	A	4.63 Å
ALA	72	A	LEU	88	A	4.76 Å
ALA	72	A	LEU	95	A	4.41 Å
ALA	72	A	ILE	97	A	4.65 Å

MET	75	A	ILE	97	A	4.30 Å
MET	75	A	ILE	99	A	3.77 Å
MET	75	A	LEU	110	A	4.23 Å
MET	75	A	ALA	114	A	4.78 Å
MET	75	A	LEU	117	A	4.56 Å
ILE	76	A	LEU	80	A	4.94 Å
ILE	76	A	ILE	86	A	4.94 Å
ILE	76	A	LEU	88	A	4.86 Å
ALA	79	A	ALA	84	A	3.96 Å
ALA	79	A	ILE	86	A	3.79 Å
ALA	79	A	ILE	99	A	4.87 Å
ALA	79	A	LEU	110	A	4.91 Å
LEU	80	A	ILE	86	A	4.54 Å
PHE	82	A	VAL	102	A	4.08 Å
PHE	82	A	VAL	106	A	4.87 Å
PHE	82	A	LEU	110	A	4.57 Å
ALA	84	A	ILE	86	A	4.45 Å
ALA	84	A	ILE	99	A	3.86 Å
ALA	84	A	VAL	102	A	4.71 Å
ILE	86	A	LEU	88	A	4.25 Å
ILE	86	A	ILE	97	A	4.90 Å
ILE	86	A	ILE	99	A	4.67 Å
LEU	88	A	LEU	95	A	4.78 Å
LEU	88	A	ILE	97	A	4.95 Å
LEU	90	A	LEU	95	A	4.43 Å
LEU	95	A	ILE	97	A	4.64 Å
ILE	97	A	ILE	99	A	4.09 Å
ILE	99	A	VAL	102	A	3.94 Å
ILE	99	A	LEU	110	A	4.97 Å
VAL	102	A	PRO	103	A	4.87 Å
VAL	102	A	VAL	106	A	3.99 Å
VAL	102	A	LEU	110	A	4.57 Å
PRO	103	A	VAL	106	A	5.00 Å
VAL	106	A	LEU	110	A	4.25 Å
ALA	114	A	VAL	125	A	4.11 Å
LEU	117	A	PHE	121	A	4.49 Å
ALA	118	A	ILE	123	A	4.19 Å
ALA	118	A	VAL	125	A	3.78 Å
PHE	121	A	ILE	123	A	4.27 Å
VAL	133	A	MET	136	A	4.44 Å
VAL	133	A	LEU	137	A	4.19 Å
VAL	133	A	ILE	160	A	4.62 Å
MET	136	A	LEU	137	A	4.84 Å
MET	136	A	VAL	140	A	4.94 Å
MET	136	A	VAL	153	A	4.21 Å
MET	136	A	ILE	160	A	4.77 Å
MET	136	A	ALA	164	A	4.53 Å
LEU	137	A	ALA	164	A	4.47 Å
VAL	140	A	ILE	151	A	4.69 Å
VAL	140	A	VAL	153	A	3.73 Å
ILE	142	A	LEU	146	A	4.53 Å
LEU	143	A	LEU	146	A	4.88 Å
LEU	143	A	ALA	148	A	4.22 Å
LEU	143	A	ILE	151	A	4.57 Å
ALA	148	A	ILE	151	A	3.79 Å
ILE	151	A	VAL	153	A	4.94 Å
VAL	153	A	ILE	160	A	4.78 Å
VAL	153	A	LEU	161	A	4.26 Å
VAL	153	A	ALA	164	A	4.35 Å

ionic (20 total):

Res1	idRes1	Ch1	Res2	idRes2	Ch2	Distance
LYS	8	A	ASP	9	A	5.91 Å
GLU	12	A	LYS	15	A	3.78 Å
GLU	18	A	ARG	22	A	5.65 Å
GLU	18	A	LYS	44	A	5.30 Å
ARG	21	A	ASP	47	A	5.51 Å
ASP	34	A	ARG	36	A	2.96 Å
GLU	40	A	LYS	43	A	2.61 Å
ARG	61	A	ASP	94	A	2.49 Å
GLU	66	A	LYS	70	A	5.38 Å
GLU	74	A	LYS	77	A	2.91 Å
GLU	104	A	ARG	107	A	5.86 Å
GLU	104	A	LYS	108	A	2.67 Å
GLU	113	A	ARG	116	A	3.23 Å
ARG	116	A	GLU	120	A	4.65 Å
GLU	135	A	LYS	138	A	4.19 Å
GLU	141	A	ARG	144	A	5.89 Å
GLU	141	A	ARG	145	A	2.88 Å
GLU	141	A	LYS	167	A	5.81 Å
ASP	157	A	ARG	159	A	4.26 Å
GLU	163	A	LYS	166	A	2.57 Å

hbond_side_side (1 total):

Res1	idRes1	Ch1	Res2	idRes2	Ch2	Distance
MET	56	A	ARG	127	A	3.37 Å

Table S–XI. Summary from ProtInter Calculator for [TFD-EE, PDB: 6ZV9].
Intermolecular Interface Interactions Between Chain A and Chain B

cationpi (2 total):

Res1	idRes1	Ch1	Res2	idRes2	Ch2	Distance
LYS	15	A	TRP	158	B	5.33 Å
TRP	158	A	LYS	15	B	5.34 Å

hydrophobic (41 total):

Res1	idRes1	Ch1	Res2	idRes2	Ch2	Distance
ILE	2	A	ALA	152	B	3.72 Å
LEU	3	A	VAL	153	B	4.87 Å
LEU	3	A	LEU	161	B	4.50 Å
LEU	3	A	ALA	164	B	4.16 Å
LEU	3	A	LEU	165	B	4.95 Å
ILE	4	A	ALA	152	B	4.18 Å
VAL	5	A	LEU	161	B	4.75 Å
ILE	19	A	TRP	158	B	4.84 Å
LEU	20	A	TRP	158	B	4.46 Å
LEU	20	A	LEU	161	B	4.82 Å
LEU	23	A	TRP	158	B	4.32 Å
LEU	23	A	LEU	165	B	4.08 Å
ALA	25	A	LEU	165	B	4.93 Å
ILE	48	A	ILE	2	B	4.61 Å
ILE	50	A	ILE	4	B	4.64 Å
LEU	69	A	LEU	80	B	3.82 Å
ILE	73	A	ILE	73	B	4.72 Å
ILE	76	A	ILE	76	B	4.38 Å
LEU	80	A	LEU	69	B	3.81 Å
LEU	80	A	LEU	88	B	4.51 Å
LEU	80	A	LEU	90	B	4.51 Å
LEU	80	A	LEU	95	B	4.15 Å
LEU	88	A	ILE	76	B	4.94 Å
LEU	88	A	LEU	80	B	4.50 Å
LEU	88	A	ILE	86	B	4.54 Å
LEU	88	A	LEU	88	B	4.77 Å
LEU	90	A	LEU	80	B	4.48 Å
LEU	95	A	LEU	80	B	4.11 Å
ALA	152	A	ILE	2	B	3.71 Å
ALA	152	A	ILE	4	B	4.18 Å
VAL	153	A	LEU	3	B	4.89 Å
TRP	158	A	ILE	19	B	4.83 Å
TRP	158	A	LEU	20	B	4.44 Å
TRP	158	A	LEU	23	B	4.31 Å
LEU	161	A	LEU	3	B	4.50 Å
LEU	161	A	VAL	5	B	4.74 Å
LEU	161	A	LEU	20	B	4.83 Å
ALA	164	A	LEU	3	B	4.17 Å
LEU	165	A	LEU	3	B	4.95 Å
LEU	165	A	LEU	23	B	4.10 Å
LEU	165	A	ALA	25	B	4.93 Å

ionic (3 total):

Res1	idRes1	Ch1	Res2	idRes2	Ch2	Distance
ASP	1	A	ARG	144	B	4.61 Å
LYS	77	A	GLU	66	B	5.98 Å
ARG	144	A	ASP	1	B	4.64 Å

Table S–XII. Summary from ProtInter Calculator for [TFD-EE MPNN, PDB: 9QUP].
Intermolecular Interactions of Chain A and Chain B

cationpi (3 total):

Res1	idRes1	Ch1	Res2	idRes2	Ch2	Distance
PHE	35	A	ARG	135	A	5.95 Å
ARG	70	A	PHE	121	A	5.23 Å
ARG	74	A	PHE	121	A	5.45 Å

hbond_main_side (10 total):

Res1	idRes1	Ch1	Res2	idRes2	Ch2	Distance
ALA	7	A	SER	32	A	2.82 Å
LEU	8	A	ARG	96	A	3.36 Å
MET	13	A	LEU	14	A	3.46 Å
SER	32	A	GLY	33	A	3.13 Å
SER	32	A	ASP	34	A	3.13 Å
ARG	65	A	GLY	92	A	3.21 Å
SER	155	A	ALA	156	A	3.12 Å
SER	155	A	ASN	157	A	2.91 Å
LEU	164	A	SER	168	A	3.18 Å
LEU	165	A	SER	168	A	2.72 Å

hydrophobic (171 total):

Res1	idRes1	Ch1	Res2	idRes2	Ch2	Distance
MET	1	A	PHE	3	A	5.00 Å
PHE	3	A	LEU	20	A	4.49 Å
PHE	3	A	ALA	25	A	4.72 Å
ILE	4	A	ALA	29	A	4.48 Å
ILE	4	A	VAL	50	A	4.72 Å
ILE	4	A	TRP	152	A	4.50 Å
VAL	5	A	ALA	7	A	4.65 Å
VAL	5	A	MET	13	A	4.67 Å
VAL	5	A	ILE	17	A	4.65 Å
VAL	5	A	LEU	20	A	4.88 Å
VAL	5	A	ILE	28	A	4.73 Å
VAL	5	A	VAL	30	A	4.58 Å
TRP	6	A	LEU	8	A	4.78 Å
ALA	7	A	MET	13	A	3.65 Å
ALA	7	A	VAL	30	A	4.85 Å
ALA	7	A	ILE	37	A	4.22 Å
LEU	8	A	ILE	37	A	4.95 Å
MET	13	A	LEU	14	A	4.71 Å
MET	13	A	ILE	17	A	4.81 Å
MET	13	A	VAL	30	A	4.48 Å
MET	13	A	ILE	37	A	4.41 Å
MET	13	A	ALA	40	A	3.87 Å
MET	13	A	ALA	41	A	4.86 Å
LEU	14	A	ILE	17	A	4.98 Å
LEU	14	A	ALA	40	A	4.91 Å
LEU	14	A	ALA	44	A	3.73 Å
ILE	17	A	ILE	28	A	4.44 Å
ILE	17	A	VAL	30	A	3.70 Å
ILE	17	A	ALA	44	A	3.91 Å
ILE	17	A	VAL	46	A	4.69 Å
LEU	20	A	ALA	25	A	4.07 Å
LEU	20	A	ILE	28	A	4.37 Å
ALA	25	A	ILE	28	A	3.92 Å
ILE	28	A	VAL	46	A	4.96 Å
ALA	29	A	VAL	50	A	4.75 Å

ALA	29	A	TRP	152	A	4.81 Å
VAL	30	A	ILE	37	A	4.44 Å
VAL	30	A	LEU	38	A	4.95 Å
VAL	30	A	ALA	41	A	3.75 Å
VAL	30	A	VAL	46	A	4.39 Å
VAL	30	A	ILE	49	A	4.05 Å
PHE	35	A	LEU	38	A	4.19 Å
PHE	35	A	VAL	51	A	4.98 Å
PHE	35	A	ALA	136	A	4.86 Å
PHE	35	A	LEU	143	A	4.36 Å
LEU	38	A	ILE	49	A	4.06 Å
LEU	38	A	VAL	51	A	4.63 Å
LEU	38	A	LEU	143	A	4.76 Å
ALA	41	A	VAL	46	A	4.11 Å
ALA	41	A	ILE	49	A	3.91 Å
ILE	42	A	ILE	49	A	3.75 Å
ILE	42	A	LEU	143	A	4.75 Å
ILE	42	A	LEU	146	A	4.54 Å
ILE	42	A	ALA	148	A	4.07 Å
VAL	46	A	ILE	49	A	4.56 Å
ILE	49	A	VAL	51	A	4.47 Å
ILE	49	A	LEU	143	A	4.59 Å
ILE	49	A	ALA	148	A	4.78 Å
VAL	50	A	TRP	152	A	4.63 Å
VAL	51	A	ILE	140	A	4.83 Å
VAL	51	A	LEU	143	A	4.22 Å
VAL	51	A	ILE	151	A	4.42 Å
VAL	51	A	VAL	153	A	4.79 Å
LEU	56	A	ILE	58	A	4.20 Å
LEU	56	A	ILE	99	A	4.46 Å
LEU	56	A	LEU	107	A	4.74 Å
LEU	56	A	LEU	110	A	4.37 Å
LEU	56	A	VAL	127	A	4.82 Å
ILE	58	A	PHE	60	A	4.78 Å
ILE	58	A	LEU	75	A	4.33 Å
ILE	58	A	VAL	97	A	4.30 Å
ILE	58	A	ILE	99	A	4.48 Å
ILE	58	A	LEU	110	A	4.99 Å
ILE	58	A	ALA	114	A	4.94 Å
ILE	58	A	VAL	125	A	4.85 Å
ILE	58	A	VAL	127	A	4.97 Å
VAL	59	A	ALA	94	A	3.82 Å
PHE	60	A	LEU	68	A	3.70 Å
PHE	60	A	ALA	71	A	4.77 Å
PHE	60	A	LEU	75	A	4.84 Å
PHE	60	A	LEU	95	A	4.28 Å
PHE	60	A	VAL	97	A	4.73 Å
PHE	60	A	ALA	114	A	4.61 Å
PHE	60	A	LEU	117	A	4.47 Å
PHE	60	A	ALA	118	A	4.87 Å
PHE	60	A	ILE	123	A	4.96 Å
PHE	60	A	VAL	125	A	4.89 Å
ALA	63	A	ALA	67	A	4.12 Å
ALA	63	A	LEU	68	A	4.93 Å
ALA	63	A	ILE	123	A	4.50 Å
ALA	67	A	PHE	121	A	4.47 Å
LEU	68	A	LEU	90	A	4.33 Å
LEU	68	A	LEU	95	A	3.95 Å
LEU	68	A	ILE	123	A	4.27 Å
ALA	71	A	PHE	121	A	4.80 Å
ALA	71	A	ILE	123	A	4.33 Å

ALA	72	A	VAL	88	A	4.09 Å
ALA	72	A	LEU	95	A	4.24 Å
ALA	72	A	VAL	97	A	4.92 Å
LEU	75	A	VAL	97	A	4.45 Å
LEU	75	A	ILE	99	A	4.26 Å
LEU	75	A	LEU	110	A	4.44 Å
LEU	75	A	LEU	113	A	4.75 Å
LEU	75	A	ALA	114	A	4.92 Å
LEU	75	A	LEU	117	A	4.22 Å
LEU	76	A	LEU	80	A	4.95 Å
LEU	76	A	VAL	86	A	4.86 Å
LEU	76	A	VAL	88	A	4.90 Å
ALA	78	A	LEU	110	A	3.72 Å
ALA	78	A	LEU	113	A	4.71 Å
ALA	79	A	ALA	84	A	3.99 Å
ALA	79	A	VAL	86	A	4.72 Å
ALA	79	A	ILE	99	A	4.50 Å
ALA	79	A	LEU	110	A	4.76 Å
LEU	80	A	VAL	86	A	4.92 Å
LEU	82	A	VAL	102	A	4.61 Å
LEU	82	A	LEU	110	A	4.14 Å
ALA	84	A	VAL	86	A	4.26 Å
ALA	84	A	ILE	99	A	3.97 Å
ALA	84	A	VAL	102	A	4.71 Å
ALA	84	A	LEU	110	A	4.95 Å
VAL	85	A	ALA	156	A	4.77 Å
VAL	86	A	VAL	88	A	3.90 Å
VAL	86	A	VAL	97	A	3.73 Å
VAL	86	A	ILE	99	A	4.73 Å
VAL	88	A	LEU	95	A	4.32 Å
VAL	88	A	VAL	97	A	4.78 Å
LEU	90	A	LEU	95	A	4.48 Å
LEU	95	A	VAL	97	A	4.27 Å
VAL	97	A	ILE	99	A	5.00 Å
ILE	99	A	VAL	102	A	4.53 Å
ILE	99	A	LEU	107	A	4.13 Å
ILE	99	A	LEU	110	A	4.63 Å
VAL	102	A	PRO	103	A	4.79 Å
VAL	102	A	LEU	107	A	4.92 Å
VAL	102	A	LEU	110	A	4.97 Å
LEU	107	A	LEU	110	A	4.96 Å
LEU	110	A	LEU	113	A	4.47 Å
LEU	113	A	LEU	117	A	4.91 Å
ALA	114	A	VAL	125	A	4.17 Å
ALA	114	A	VAL	127	A	4.16 Å
LEU	117	A	PHE	121	A	4.85 Å
ALA	118	A	ILE	123	A	4.31 Å
ALA	118	A	VAL	125	A	3.90 Å
PHE	121	A	ILE	123	A	4.62 Å
VAL	125	A	VAL	127	A	4.71 Å
PRO	133	A	TRP	160	A	4.87 Å
PRO	133	A	LEU	164	A	4.16 Å
PRO	133	A	LEU	167	A	3.80 Å
ALA	136	A	ILE	140	A	4.82 Å
ALA	136	A	TRP	160	A	4.75 Å
ALA	136	A	LEU	164	A	4.47 Å
LEU	137	A	ILE	140	A	4.82 Å
LEU	137	A	LEU	164	A	4.49 Å
LEU	137	A	LEU	167	A	4.70 Å
ILE	140	A	ILE	151	A	4.51 Å
ILE	140	A	VAL	153	A	4.78 Å

ILE	140	A	LEU	164	A	4.80 Å
LEU	143	A	LEU	146	A	4.43 Å
LEU	143	A	ALA	148	A	4.37 Å
LEU	143	A	ILE	151	A	4.38 Å
ALA	148	A	ILE	151	A	4.14 Å
ILE	151	A	VAL	153	A	4.43 Å
VAL	153	A	TRP	160	A	4.77 Å
VAL	153	A	LEU	161	A	4.58 Å
VAL	153	A	LEU	164	A	4.07 Å
VAL	158	A	LEU	161	A	4.87 Å
VAL	158	A	LEU	162	A	4.82 Å
TRP	160	A	LEU	161	A	4.83 Å
TRP	160	A	LEU	164	A	4.73 Å
LEU	162	A	LEU	165	A	4.92 Å

ionic (19 total):

Res1	idRes1	Ch1	Res2	idRes2	Ch2	Distance
LYS	10	A	ASP	11	A	4.08 Å
LYS	15	A	GLU	18	A	5.43 Å
GLU	18	A	LYS	22	A	2.82 Å
ASP	34	A	ARG	96	A	5.55 Å
ASP	34	A	ARG	128	A	5.08 Å
ASP	36	A	ARG	39	A	3.73 Å
ASP	36	A	ARG	128	A	5.50 Å
ARG	39	A	GLU	43	A	4.66 Å
GLU	47	A	LYS	149	A	2.66 Å
ASP	64	A	ARG	70	A	5.41 Å
ARG	74	A	GLU	120	A	5.82 Å
ASP	91	A	ARG	96	A	4.87 Å
GLU	104	A	ARG	111	A	4.40 Å
ASP	106	A	ARG	109	A	4.42 Å
GLU	108	A	ARG	111	A	3.85 Å
GLU	108	A	ARG	115	A	5.22 Å
GLU	126	A	ARG	128	A	3.68 Å
GLU	134	A	LYS	163	A	5.65 Å
ARG	135	A	GLU	139	A	5.20 Å

hbond_side_side (1 total):

Res1	idRes1	Ch1	Res2	idRes2	Ch2	Distance
SER	52	A	ARG	98	A	3.34 Å

Table S–XIII. Summary from ProtInter Calculator for [TFD-EE MPNN, PDB: 9QUP].
Intermolecular Interface Interactions Between Chain A and Chain B

hydrophobic (56 total):

Res1	idRes1	Ch1	Res2	idRes2	Ch2	Distance
MET	1	A	ILE	140	B	4.99 Å
MET	1	A	ILE	151	B	4.84 Å
MET	1	A	VAL	153	B	4.91 Å
MET	1	A	LEU	164	B	4.17 Å
PHE	3	A	VAL	153	B	4.90 Å
PHE	3	A	LEU	161	B	4.88 Å
PHE	3	A	LEU	164	B	4.63 Å
PHE	3	A	LEU	165	B	4.78 Å
VAL	5	A	LEU	161	B	4.93 Å
TRP	6	A	VAL	85	B	4.56 Å
TRP	6	A	ALA	156	B	4.48 Å
ALA	19	A	VAL	158	B	4.23 Å
ALA	19	A	LEU	162	B	4.82 Å
LEU	20	A	VAL	158	B	4.00 Å
LEU	20	A	LEU	161	B	4.87 Å
LEU	20	A	LEU	162	B	4.98 Å
LEU	20	A	LEU	165	B	4.99 Å
ALA	23	A	LEU	162	B	4.92 Å
ALA	23	A	LEU	165	B	4.64 Å
ALA	25	A	LEU	165	B	4.66 Å
VAL	50	A	ILE	4	B	4.79 Å
ALA	72	A	LEU	76	B	4.89 Å
ALA	72	A	LEU	80	B	4.59 Å
LEU	76	A	LEU	76	B	4.45 Å
LEU	80	A	VAL	88	B	4.81 Å
LEU	80	A	LEU	90	B	4.28 Å
LEU	80	A	LEU	95	B	4.77 Å
VAL	85	A	TRP	6	B	4.74 Å
VAL	85	A	ALA	89	B	4.81 Å
VAL	88	A	LEU	76	B	4.21 Å
VAL	88	A	LEU	80	B	4.95 Å
ALA	89	A	VAL	85	B	4.71 Å
LEU	90	A	LEU	80	B	4.56 Å
LEU	95	A	LEU	80	B	4.41 Å
LEU	137	A	MET	1	B	4.86 Å
ILE	140	A	MET	1	B	4.95 Å
ILE	151	A	MET	1	B	4.83 Å
TRP	152	A	ILE	4	B	4.54 Å
TRP	152	A	TRP	152	B	4.78 Å
VAL	153	A	MET	1	B	4.87 Å
VAL	153	A	PHE	3	B	4.96 Å
ALA	156	A	TRP	6	B	4.69 Å
VAL	158	A	ALA	19	B	4.76 Å
VAL	158	A	LEU	20	B	3.92 Å
LEU	161	A	PHE	3	B	4.03 Å
LEU	161	A	VAL	5	B	4.49 Å
LEU	161	A	LEU	20	B	4.90 Å
LEU	162	A	ALA	19	B	4.87 Å
LEU	162	A	LEU	20	B	4.34 Å
LEU	162	A	ALA	23	B	4.88 Å
LEU	164	A	MET	1	B	4.23 Å
LEU	164	A	PHE	3	B	4.61 Å
LEU	165	A	PHE	3	B	4.28 Å
LEU	165	A	LEU	20	B	4.76 Å
LEU	165	A	ALA	23	B	4.88 Å

LEU	165	A	ALA	25	B	4.92 Å

ionic (7 total):

Res1	idRes1	Ch1	Res2	idRes2	Ch2	Distance
ARG	69	A	ASP	77	B	3.88 Å
ARG	69	A	GLU	81	B	5.04 Å
LYS	73	A	ASP	77	B	4.86 Å
ASP	77	A	ARG	69	B	3.22 Å
ASP	77	A	LYS	73	B	3.70 Å
GLU	81	A	ARG	65	B	4.89 Å
GLU	81	A	ARG	69	B	3.52 Å

S8–REFERENCES

1. Chiu, J., et al., *Site-directed, Ligase-Independent Mutagenesis (SLIM): a single-tube methodology approaching 100% efficiency in 4 h.* Nucleic acids research, 2004. **32**(21): p. e174-e174.
2. McGibbon, R.T., et al., *MDTraj: a modern open library for the analysis of molecular dynamics trajectories.* Biophysical journal, 2015. **109**(8): p. 1528-1532.
3. Gowers, R.J., et al., *MDAnalysis: a Python package for the rapid analysis of molecular dynamics simulations*. 2019, Los Alamos National Laboratory (LANL), Los Alamos, NM (United States).
4. Michaud-Agrawal, N., et al., *MDAnalysis: a toolkit for the analysis of molecular dynamics simulations.* Journal of computational chemistry, 2011. **32**(10): p. 2319-2327.
5. Janin, J., et al., *Conformation of amino acid side-chains in proteins.* Journal of molecular biology, 1978. **125**(3): p. 357-386.
6. Case, D.A., et al., *AmberTools.* Journal of chemical information and modeling, 2023. **63**(20): p. 6183-6191.
7. Valdés-Tresanco, M.S., et al., *gmx_MMPBSA: a new tool to perform end-state free energy calculations with GROMACS.* Journal of chemical theory and computation, 2021. **17**(10): p. 6281-6291.